

**Analytical Model for Chromatic Dispersion and Dispersion Slope
Compensation Using Linearly Chirped Apodized Fiber Bragg Grating**

by
Sher Shermin Azmiri Khan

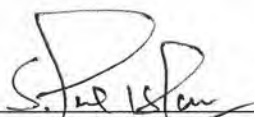
**MASTER OF SCIENCE IN
INFORMATION AND COMMUNICATION TECHNOLOGY**

**Institute of Information and Communication Technology
BANGLADESH UNIVERSITY OF ENGINEERING AND TECHNOLOGY (BUET)**

2012


The thesis entitled “Analytical Model for Chromatic Dispersion and Dispersion Slope Compensation Using Linearly Chirped Apodized Fiber Bragg Grating,” submitted by **Sher Shermin Azmiri Khan**, Roll No: M10063123P, Session: October 2006 has been accepted as satisfactory in partial fulfillment of the requirement for the degree of **Master of Science in Information and Communication Technology** on 29 September 2012.

BOARD OF EXAMINERS




Dr. Md. Saiful Islam
Professor
IICT, BUET
Dhaka 1000, Bangladesh

Chairman
(Supervisor)




Dr. Md. Saiful Islam
Professor and Director
IICT, BUET
Dhaka 1000, Bangladesh

Member
(Ex-officio)



Dr. Md. Liakot Ali
Professor
IICT, BUET
Dhaka 1000, Bangladesh

Member



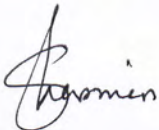
Dr. Mohammad Rakibul Islam
Professor
Department of EEE
Islamic University of Technology
Board Bazar, Gazipur, Bangladesh

Member
(External)

CANDIDATE'S DECLARATION

It is hereby declared that this thesis entitled “**Analytical Model for Chromatic Dispersion and Dispersion Slope Compensation Using Linearly Chirped Apodized Fiber Bragg Grating,**” or any part of it has not been submitted elsewhere for the award of any degree or diploma.

Signature of the candidate



Sher Shermin Azmiri Khan

Roll No: M10063123P

Dedicated to
My Parents, Father and Mother In-Laws,
Husband and Daughter

Table of Contents

List of Tables	viii
List of Figures	ix
List of Abbreviations	xii
List of Symbols	xiii
Acknowledgment	xv
Abstract	xvi
Chapter 1	1
Introduction	
1.1 Introduction	1
1.2 Literature Review	2
1.3 Objectives of the Work	5
1.4 Methodology	5
1.5 Organization of the Thesis	6
Chapter 2	7
Fiber Bragg Grating and Dispersion	
2.1 Introduction	7
2.2 Grating Structure	7
2.2.1 Uniform Index Change FBG	8
2.2.2 Chirped FBG	8
2.2.3 Apodized FBG	11
2.2.4 Tilted Fiber Bragg Gratings	12
2.2.5 Long-period Gratings	13

2.3 Application of Fiber Bragg Gratings	13
2.4 Dispersion in Singlemode Fiber	14
2.5 Chromatic Dispersion	14
2.6 Group Velocity Dispersion	16
2.7 Summary	18
Chapter 3	19
Theoretical Analysis	
3.1 Introduction	19
3.2 System Model	19
3.3 Pulse Broadening Factor in Dispersive Fiber	20
3.4 Phase of Reflectivity and Time Delay of FBG	25
3.5 Analytical Formulation for Dispersion Derivation	28
3.6 Apodization Profiles	30
3.7 Design Consideration of Linearly Chirped Grating Period	32
3.8 Typical Optical Transmission System	32
3.9 Summary	34
Chapter 4	35
Experimental Result Analysis	
4.1 Introduction	35
4.2 Determination of Appropriate Apodization Function	36
4.3 Determination of FBG Grating Length	42
4.4 Dispersion Compensation	48
4.5 Comparison with Contemporary Works	61

4.6	Summary	64
Chapter 5		65
Conclusions		
5.1	Conclusion	65
5.2	Future Scopes	66
References		68
List of Publications		71

List of Tables

Table Number	Titles of the Tables	Page Number
4.1	Parameter values use for theoretical calculation	35
4.2	Relationship between fiber Bragg grating's grating length and reflectivity	45

List of Figures

Figure Number	Captions of the Figures	Page Number
2.1	Schematic diagram of a FBG illustrating that only the wavelength of light, λ_B , that satisfies the Bragg condition, is reflected.	8
2.2	Response of chirped Bragg grating, where a) Illustration of the spectral response of the chirped grating and b) The variation of the resonance condition with grating length	9
2.3	Illustration of the chirped FBG with position detuned Bragg wavelength where the detuning is, a) driven by the position dependence periodicity, $\Lambda(z)$ and b) is driven by the varying mode index with position $n_{eff}(z)$.	11
2.4	Total dispersion D and relative contributions of material dispersion (MD) and wave-guide dispersion (WD) for a conventional single-mode fiber.	15
3.1	System model of dispersion compensation	20
3.2	A block diagram of an typical optical communication system.	33
3.3	Dispersion Compensation using FBG	33
4.1	Reflection spectrum of <i>tanh</i> profile for $\alpha=1, \beta=4$	37
4.2	Reflection spectrum of hamming profile for $H=0.8$	37
4.3	Reflection spectrum of Gauss profile for $G=0.5$	38
4.4	Reflection spectrum of <i>cosine</i> profiles for $A=0.15$	38
4.5	Reflection spectrum of <i>Cauchy</i> profile for $B=0.2$	39
4.6	Reflection spectrum of <i>sinc</i> profile for $X=1, Y=3$	39
4.7	Reflection spectrum of <i>tanh</i> ($\alpha=1, \beta=4$), hamming ($H=0.8$), Gauss ($G=0.5$), <i>cosine</i> ($A=0.15$), <i>Cauchy</i> ($B=0.2$), <i>sinc</i> ($X=1, Y=3$) apodization profiles	40
4.8	Grating length versus apodization strength for <i>tanh</i> ($\alpha=1, \beta=4$), hamming ($H=0.8$), Gauss ($G=0.5$), <i>cosine</i> ($A=0.15$), <i>Cauchy</i> ($B=0.2$), <i>sinc</i> ($X=1, Y=3$) apodization profiles for 110 km of fiber length	41
4.9	Apodization function versus normalized length for <i>Tanh</i> ($\alpha=1, \beta=4$), Hamming ($H=0.8$), Gauss ($G=0.5$), <i>Cosine</i> ($A=0.15$), <i>Cauchy</i> ($B=0.2$), <i>sinc</i> ($X=1, Y=3$).	42

4.10	Reflectivity versus wavelength for 4 cm of grating length for <i>sinc</i> profile	43
4.11	Reflectivity versus wavelength for 7 cm of grating length for <i>sinc</i> profile	44
4.12	Reflectivity versus wavelength for 10 cm of grating length for <i>sinc</i> profile	44
4.13	Reflectivity versus wavelength for 12 cm of grating length for <i>sinc</i> profile	45
4.14	The relationship between reflectivity and grating length for <i>sinc</i> profile	47
4.15	The relationship between reflectivity and grating length for <i>tanh</i> ($\alpha=1$, $\beta=4$), hamming ($H=0.8$), Gauss ($G=0.5$), <i>cosine</i> ($A=0.15$), <i>Cauchy</i> ($B=0.2$), <i>sinc</i> ($X=1$, $Y=3$) apodization profiles	47
4.16	Dispersion coefficient versus wavelength using linearly chirped <i>sinc</i> apodized FBG for different grating length	48
4.17	Linearly chirped grating period (with 200 segment, length of 1 st period is 1.6 mm, and linearly decrease by a factor of 0.99 mm) versus Bragg wavelength	49
4.18	2 nd order dispersion (β_2) versus wavelength using linearly chirped <i>sinc</i> apodized FBG	50
4.19	3 rd order dispersion (β_3) versus wavelength using linearly chirped <i>sinc</i> apodized FBG	50
4.20	Pulse broadening factor in SSMF fiber as a function of link length operating at bit rates 10 Gbps and 40 Gbps with 60 mW input power considering the effect of β_2	51
4.21	Pulse broadening factor in SSMF fiber as a function of link length operating at bit rates 10 Gbps with 60 mW input power considering both β_2 and β_3	52
4.22	Pulse broadening factor in SSMF fiber as a function of link length operating at bit rates 40 Gbps with 60 mW input power considering both β_2 and β_3	53
4.23	Pulse broadening factor in SSMF fiber is as a function of link length operating at bit rates 10 Gbps with 60 mW input power before and after cascading FBG in fiber link length.	54
4.24	Pulse broadening factor in SSMF fiber is as a function of link length operating at bit rates 40 Gbps with 60 mW input power before and after cascading FBG in fiber link length.	55
4.25	Analytically calculated dispersion coefficient versus wavelength using linearly chirped <i>sinc</i> apodized FBG	56

4.26	Analytically calculated dispersion slope versus wavelength using linearly chirped <i>sinc</i> apodized FBG	57
4.27	Dispersion coefficients versus wavelength for unapodized FBG and sinc apodized FBG	58
4.28	Reflectivity spectra of a WDM system by using proposed dispersion compensation grating	59
4.29	Initial, broadened and recompressed pulse after transmission through 100 km of fiber and 10 cm of fiber Bragg grating. Data rate 10 Gbps. Input power 60 mW	60
4.30	Initial, broadened and recompressed pulse after transmission through 100 km of fiber and 10 cm of fiber Bragg grating. Data rate 40 Gbps.	60
4.31	Comparison between numerically calculated value with analytical model for dispersion coefficients versus wavelength	61
4.32	Comparison of simulation results of this work with the already published data in [5]	62
4.33	Comparison of simulation results of this work with experimental data the already published in [13]	63

List of Abbreviations

AFBG	Apodized Fiber Bragg Gratings
CCRC	Canadian Communications Research Center
CD	Chromatic Dispersion
CFBG	Chirped Fiber Bragg Grating
CME	Coupled Mode Equations
DSF	Dispersion Shifted Fiber
EMI	Immune to Electromagnetic Interference
FBG	Fiber Bragg Gratings
FWHM	Full Width at Half Maximum
GVD	Group Velocity Dispersion
LCFBG	Linearly Chirped Fiber Bragg gratings
LED	Light Emitting Diodes
MD	Material Dispersion
NLSE	Nonlinear Schrödinger Equation
PMD	Polarization Mode Dispersion
PUA	Piecewise Uniform Approach
RKM	Runge Kutta Method
RMS	Root Mean Square
SSMF	Standard Single Mode Fiber
TFBG	Tilted Fiber Bragg Gratings
UV	Ultraviolet
WD	Wave-guide Dispersion
WDM	Wavelength Division Multiplexed

List of Symbols

τ	Pulse Width of a Sample
λ	Wavelength
λ_B	Bragg wavelength
n_{eff}	Effective index
Λ	Grating period
z	Position along the grating
n	Mode index
f	Fundamental Frequency
ω	Angular frequency
D	Chromatic dispersion
D_M	Material dispersion
D_w	Waveguide dispersion
S_0	Zero dispersion slope
Δt	Pulse spreading
β_1	1 st order dispersion
β_2	2 nd order dispersion
β_3	3 rd order dispersion
M	Modulation Index
$\hat{\sigma}$	“dc” self-coupling coefficient
κ	“ac” coupling coefficient
ρ	Amplitude of reflection coefficient
r	Power reflection coefficient
τ_p	Delay time

d_p	Second order dispersion
δ	Detuning
n	Sample Number
p	Number of Poles per Phase of the Motor
$T(z)$	Apodization profile/function
a_{eff}	Apodization factor
M	Linear change of phase
N	Number of grating period.
L_g	Gating length
T	Fundamental Time Period

ACKNOWLEDGEMENTS

First of all, the author expresses her heartiest gratitude to the Almighty Allah, the most beneficent, the most merciful to give her “toufique” to complete this work successfully.

Then the author expresses her profound gratitude and respect to her supervisor Dr. Md. Saiful Islam, Professor of the Institute of Information and Communication Technology (IICT), Bangladesh University of Engineering and Technology (BUET), for his erudite suggestions, helpful discussions, invaluable assistance and great encouragement in the process of completing this work. Without his able guidance, constructive suggestions, supply of research materials and above all wholehearted supervision it would have been impossible to realize the work in time.

Finally, the author expresses her profound gratitude to her parents, husband, daughter and the other family members for their sacrifices, inspiration and extension of their hands during the progress of this work, especially to her father and mother in-laws for keeping aside her from the family duties and responsibilities during the entire period of her graduate studies.

ABSTRACT

Chromatic dispersion (CD) is a phenomenon caused by wavelength dependent group velocity of an optical signal which travels at slightly different speeds in an optical fiber and leads to inter-symbol interference that eventually results in data loss and traffic interruption. As bit rates of optical fiber communication are increased, CD and dispersion slope also increase and hence it creates a big problem to transmit the data. The traditional means of decreasing the CD and dispersion slope by the deployment of dispersion compensating fiber (DCF) bundles throughout the optical network. Insertion loss and nonlinearity are the main drawbacks of using DCF for CD and dispersion slope compensation. CD and dispersion slope compensation using reflective Fiber Bragg Grating (FBG) is technically sound and cost effective. FBGs are also compact and provide no nonlinearity. In this thesis, an attempt is made to develop analytical models for CD and dispersion slope compensator using linearly chirped FBG by suppressing the reflected side lobes. Side lobes of the FBGs limit the CD compensation performance and introduce noise in the transmission system. Apodization is usually used to suppress the side lobes. Different apodization functions are compared to find out the best fit for CD compensation. It is found that the *sinc* apodization function is the most appropriate function to achieve significant negative dispersion in terms of strength factor and FBG length. Results show that a 10 cm FBG provides maximum negative dispersion (-70 ps/nm) and dispersion slope (-9 ps/nm²) at 1558 nm wavelength. Using the developed models MATLAB simulation is carried out to compensate CD for an optical transmission of various link length, input power and bit rate. The analysis and findings of this thesis will be helpful in designing appropriate dispersion compensation mechanism in modern high bit rate optical transmission system.

Chapter 1

Introduction

1.1 Introduction

As data rates of telecom systems increase, new technical challenges appear, including the adverse effects of signal broadening caused by chromatic dispersion. This physical phenomenon originates from the wavelength dependence of the propagation velocity in the transport optical fiber. In such a material, the shorter part of an optical pulse propagates faster than its larger part, resulting in progressive pulse broadening.

Fortunately, it is easy to recompress the optical pulses by providing a device that does just the opposite: providing a longer propagation time for the shorter part than for the larger part of the optical pulses. This scheme is referred to as dispersion compensation. For example, dispersion-shifted fiber (DSF) was developed to provide negligible chromatic dispersion, but brings new problems, and DCFs suffer from high insertion loss and sensitivity to nonlinear effects.

A fiber Bragg grating (FBG) is a type of distributed Bragg reflector constructed in a short segment of optical fiber that reflects particular wavelengths of light and transmits all others. This is achieved by adding a periodic variation to the refractive index of the fiber core, which generates a wavelength specific dielectric mirror. A FBG can therefore be used as a dispersion compensator in a communication link. FBG is small in size, has less insertion loss and has no nonlinear effect.

FBG can be fabricated by exposing the core of the optical fiber to UV radiation. This induces refractive index change along the core of the fiber. It is believed that there will be an increased use of such devices in wavelength-division-multiplexed (WDM) systems,

channel selection, deployment of transmitters in the upstream path in a network, and viable routing schemes, amongst others. The fascinating technology of a simple in-line, all-fiber optical filter is based on the principle of photosensitive fiber.

This thesis is focused on investigating and developing an analytical model of a linearly chirped apodized FBG for dispersion compensation.

1.2 Literature Review

Dispersion is the time domain spreading of light pulse as it travels through the fiber. The optical pulse is made of more than one wavelength component. Each component travels at slightly difference speed which results spreading of the output pulse and is termed as chromatic dispersion (CD) [1]. Over the years many methods and techniques were developed to compensate dispersion but linearly chirped FBG plays a special role to compensate CD in optical links [2]. Here we have reviewed some of the previous works.

Bandyopadhyay et al studied apodized linearly chirped fiber FBGs with a view of determining an optimal set of grating parameters to design and fabricate linear edge filter for Bragg grating. The response characteristics of the transition edges of symmetric CFBGs have been evaluated thoroughly [3].

Bragg wavelength shift is numerically studied for different apodization profiles of chirped FBG. Linear and nonlinear cases are modeled and investigated. Effects of temperature, pressure and strain under the sea level are studied together with the effect of nonlinearity [4].

Chai et al investigated the effect of apodization parameter on performance of the linearly chirped FBG for dispersion compensation. Use of appropriate apodization parameter minimizes the effect of side lobes [5]. They have considered only the dispersion not the dispersion slope.

S. Doucet et al described in details the design and fabrication of a tunable chromatic

dispersion equalizer based on phase apodized FBGs in [6]. This paper has discussed in detail the numerical techniques used in the optimization of the fiber Bragg grating. It shows that the use of a low chirp results in the distribution of the resonating cavities along the optical fiber length, which allows reconfiguration of the spectral characteristics by the application of a temperature profile.

Li et al show a novel approach for the simultaneous CD and its slope compensation using phase only sampled FBG [7]. The sampling-function is used with an analytical form with a linearly-chirped sampling period and is optimized by using the simulated annealing algorithm. But phase-only sampled FBG is not easy to fabricate because of availability of phase-mask. Moreover, their solution is based on an assumption that the grating is extremely strong, which is unrealistic for a high channel-count FBG due to the limited index change that is difficult to attain.

Ho et al perform a modeling, simulation and characterisation of FBG with different grating lengths. It is shown that the grating length represents as one of the critical parameters in contributing to a high performance FBG [8].

FBG length and its apodization also plays a critical role in controlling CD and Hany et al. demonstrated tunable dispersion compensation both experimentally and numerically with chirped apodized FBG when operated in transmission [9]. Comparison between the results of strain and temperature dependent center Bragg wavelength shift have been accomplished using different apodization profiles to produce linearly chirped apodized far off resonance fiber Bragg gratings for the design of an optimum dispersion compensator. Dispersion slope is the limitation of this system performance.

Gualda et al have presented a scheme to enhance the performance of an ultra high capacity (100Gb/s) long haul transmission system that makes use of chirped FBG for dispersion slope compensation [10]. It is shown that the FBG effectively compensate the dispersion slope while there present a penalty to the system performance due to unwanted group delay ripple.

The electric arc technique is used to fabricate an apodized FBGs. Arc discharges applied to the ends of the grating produce a smoothing of the refractive index modulation profile reducing the sidelobes of the reflection spectrum at longer wavelengths [11].

Hany et al have discussed the use of apodized FBGs, operated in transmission, as dispersion compensators using a far more flexible and controllable approach to chirped grating fabrication relying on two beam interference and is based on the use of dissimilar curvatures in the interfering wave fronts [12]. This is accomplished by placing two lenses in the two arms of an interferometer. Different apodization profiles and design parameters are studied showing their effects on the performance of the compensator.

Single FBG designed to compensate for pure third order dispersion are demonstrated in [13]. The experimental achievement of single gratings with broad spectral bandwidth profiles and pure dispersion slope compensation abilities has been demonstrated. The demonstrated gratings require maximum index modulations together with full control of both phase and amplitude.

N. H. Sunand et al demonstrate both single and multi channel 40-Gb/s tunable dispersion compensation using nonlinearly chirped FBGs. An experimental work has been done for both single channel and multi channel systems. It shows a wide tuning range for 40 Gb/s, negligible intra channel third-order dispersion, and both positive and negative dispersion values.

From the above discussion and literature review, we have observed that most of the research works have been done to analyze different performance of FBGs for dispersion or dispersion slope compensation through analytical simulation or experimental study. But no work is reported yet that formed a complete analytical model considering all FBG parameters for simultaneous dispersion and dispersion-slope compensation based on a linearly chirped apodized FBG. Choosing appropriate apodization profile for a particular application is a tedious task. In this research work an analytical model for CD

and dispersion slope compensation has been developed using appropriate chirped apodized FBG.

1.3 Objectives of the Work

Dispersion compensation management plays a critical role in the over all performance of an optical transmission system. The main goal of this research is to compensate CD and dispersion slope simultaneously using apodized FBG. The following objectives are identified:

- i) To develop an analytical expression for pulse broadening factor due to CD and dispersion slope.
- ii) To study and compare different apodization profiles of linearly chirped FBG to find out the appropriate profile for CD compensation.
- iii) To develop an analytical model based on linearly chirped FBG to compensate CD and dispersion slope simultaneously.
- iv) To compare the performance of the compensator with existing other methods.

1.4 Methodology

First of all, pulse spreading by the dispersive effects of the fiber is studied. An analytical formulation is developed to calculate the effect of pulse broadening considering the CD and its slope impairments.

Secondly, appropriate apodization strength factor range is determined considering the effect of link length. Different apodization functions also compared to find out the optimal one.

Thirdly, an analytical model for nonlinear chirped FBG is developed for the dispersion and dispersion slope compensation. A mathematical relationship is established for the linearly chirp grating period of FBG .The shorter wavelength gets reflected back quickly and longer wavelength take longer time to reflect as it penetrates more distance in FBG.

Then analytical model is developed to calculate the delay of FBG. Analytical models for 1st order dispersion and 2nd order dispersion of FBG are also developed. Thus broadened pulse due to CD and its slope can be recompressed by inserting proposed FBG in the appropriate position of fiber optic transmission system.

Finally, numerical simulation is carried out by MATLAB software using the derived equations. Performance of the proposed compensator is compared with the other existing methods.

1.5 Organization of the Thesis

This thesis is organized as follows.

Chapter 2 reviews the historical background of fiber Bragg grating and different grating structure. It also provides some application of FBG. After that, it elucidates how dispersion in a single mode fiber occurred. Then it explains group velocity dispersion.

Chapter 3 discusses about analytical and simulation modeling of FBG. Pulse broadening factor is derived. Also the phase of reflectivity and delay time of FBG is also explored analytically. It then presents a proposed model for linearly chirped apodized FBG for dispersion compensation.

Chapter 4 provides MATLAB simulation results of the developed models proposed in chapter 2 and explores the effects of the variation of the different apodization profiles. It also explains the simulated results.

Finally, Chapter 5 concludes the thesis with a summary, and few suggestions for the future scopes of this work.

Chapter 2

Fiber Bragg Gratings and Dispersion

2.1 Introduction

A fiber Bragg grating (FBG) is a type of distributed Bragg reflector constructed in a short segment of optical fiber that reflects particular wavelengths of light and transmits all others. This is achieved by adding a periodic variation to the refractive index of the fiber core, which generates a wavelength specific dielectric mirror. A FBG can therefore be used as an inline optical filter to block certain wavelengths, or as a wavelength-specific reflector.

FBG is proving to be one of the most important developments in the field of the optical fiber technology. FBGs are used in optical communication links in different applications such as all-optical routers, selective filters, gain equalizers, sensors and dispersion compensators. These are generalized distributed reflectors whose reflection spectra and dispersion characteristics are wavelength dependent and can be accurately adjusted by proper design.

2.2 Grating Structure

The structure of the FBG can vary via the refractive index, or the grating period. The grating period can be uniform or graded, and either localized or distributed in a superstructure. The refractive index has two primary characteristics, the refractive index profile, and the offset. Typically, the refractive index profile can be uniform or apodized, and the refractive index offset is positive or zero.

There are some common structures for FBGs;

- Uniform index change FBG,
- Chirped FBG,
- Apodized FBG
- Tilted FBG
- Long-period FBG.

2.2.1 Uniform Index Change FBG

For a uniform FBG, the period Λ remains constant throughout the length and the reflection is the strongest at the Bragg wavelength, λ_B . The Bragg resonant wavelength is a function of the period, Λ and the mode effective index (n_{eff}) which is given by [23];

$$\lambda_B = 2n_{eff}\Lambda_B \quad (2.1)$$

Light at the Bragg wavelength, λ_B , propagates in the fibre undergoes reflection and the rest of the light is transmitted through the grating unimpeded. The spectral characteristics depend on the grating's parameters, such as the amplitude of the refractive modulations, grating length, the coupling strength and the overlap integral of the forward and backward propagating modes. A typical reflection spectrum of a uniform FBG is shown in Fig. 2.1.

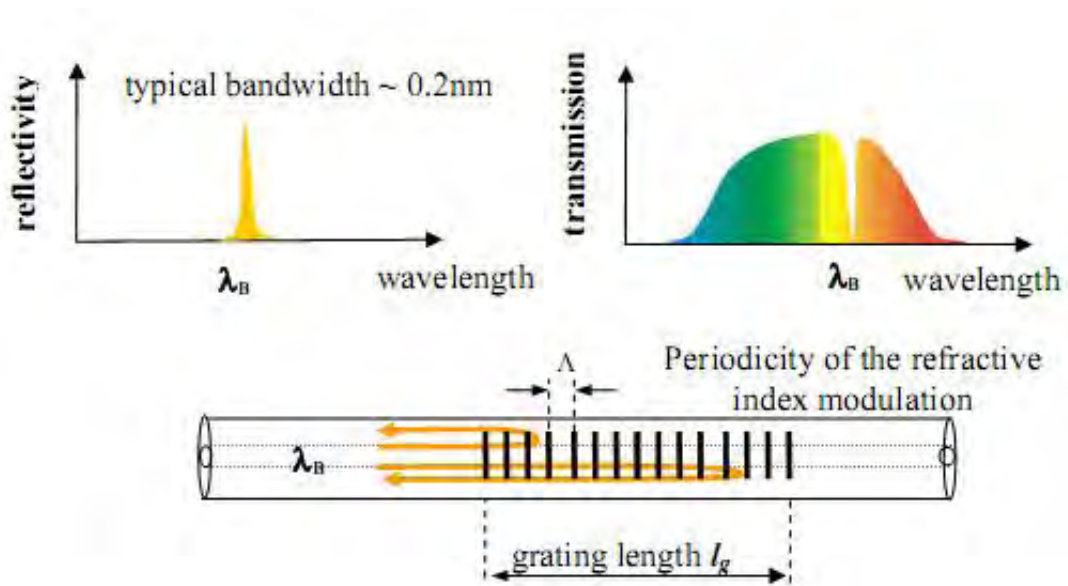


Fig. 2.1 Schematic diagram of a uniform FBG illustrating that only the wavelength of light, λ_B , that satisfies the Bragg condition, is reflected.

2.2.2 Chirped FBG

A chirped FBG has a Bragg condition, equation (2.1) which varies as a function of position along the grating. This is achieved by ensuring that the periodicity, Λ , varies as a function of position, or that the mode index, n_{eff} varies as a function of position along the FBG [22, 23],

or through a combination of both. The Bragg condition for the chirp FBGs can be written as in equation (2.2).

$$\lambda_B(z) = 2n_{eff}(z)\Lambda_B(z) \quad (2.2)$$

,where z is the position along the grating. With this type of structure, the resonance condition is no longer localized but is position dependent. Each position has its' own resonance condition and reflects its own wavelength. This can also be interpreted as each wavelength having a different reflection point along the grating. The chirp in the FBG's period gives rise to a broadened reflected spectrum as illustrated in Fig. 2.2.

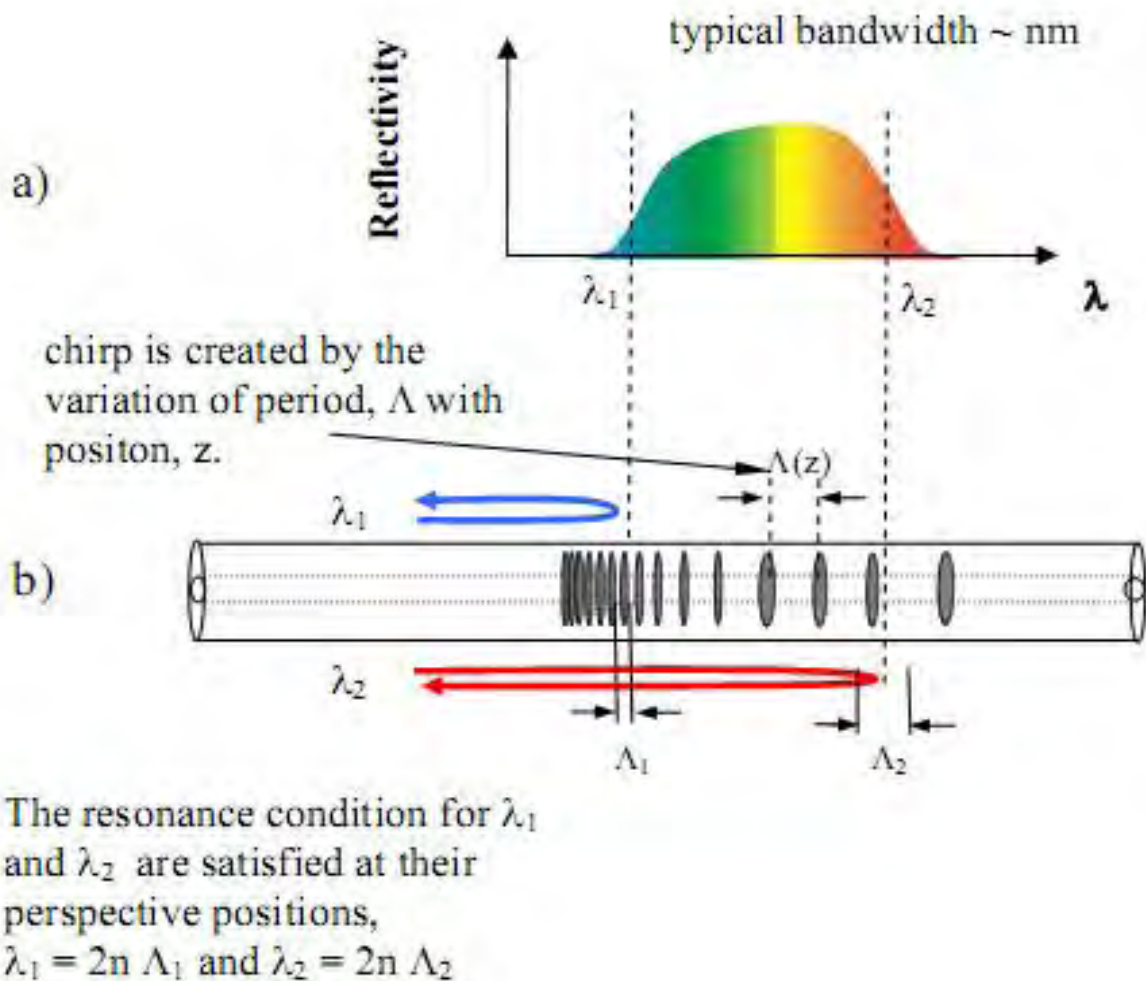


Fig. 2.2 Response of chirped Bragg grating, where a) Illustration of the spectral response of the chirped grating and b) The variation of the resonance condition with grating length.

The wider bandwidth offered by chirp FBGs provides a larger spectral range to operate within. In a linearly periodic chirped FBG, the dependence of the period of the refractive modulation upon the axial position along the FBG can be expressed as [26];

$$\Lambda(z) = \Lambda_0 + \frac{(\Lambda_{l_g} - \Lambda_0)}{l_g} z \quad (2.3)$$

,where Λ_0 is the period at the start of the grating, Λ_{l_g} is the period at the end of the grating and l_g is the grating length. The equation (2.3) describing the dependence of periodicity upon position is illustrated in Fig. 2.2 (a). This provides a varying Bragg condition along the length of the grating.

The resonance condition is also dependent on the mode index. This provision of chirp in the FBG can also be realized by creating a varying mode index along the length of the FBG. Figure 2.2 (b) demonstrates how a variation in Bragg wavelength with position is possible by introducing a mode index variation with grating length while keeping the periodicity constant. The dependence of the mode refractive index upon the axial position along the FBG can be written similarly to equation (2.3);

$$n(z) = n_0 + \frac{(n_{l_g} - n_0)}{l_g} z \quad (2.4)$$

,where n_0 is the mode index at the start of the grating, n_{l_g} is the mode index at the end of the grating.

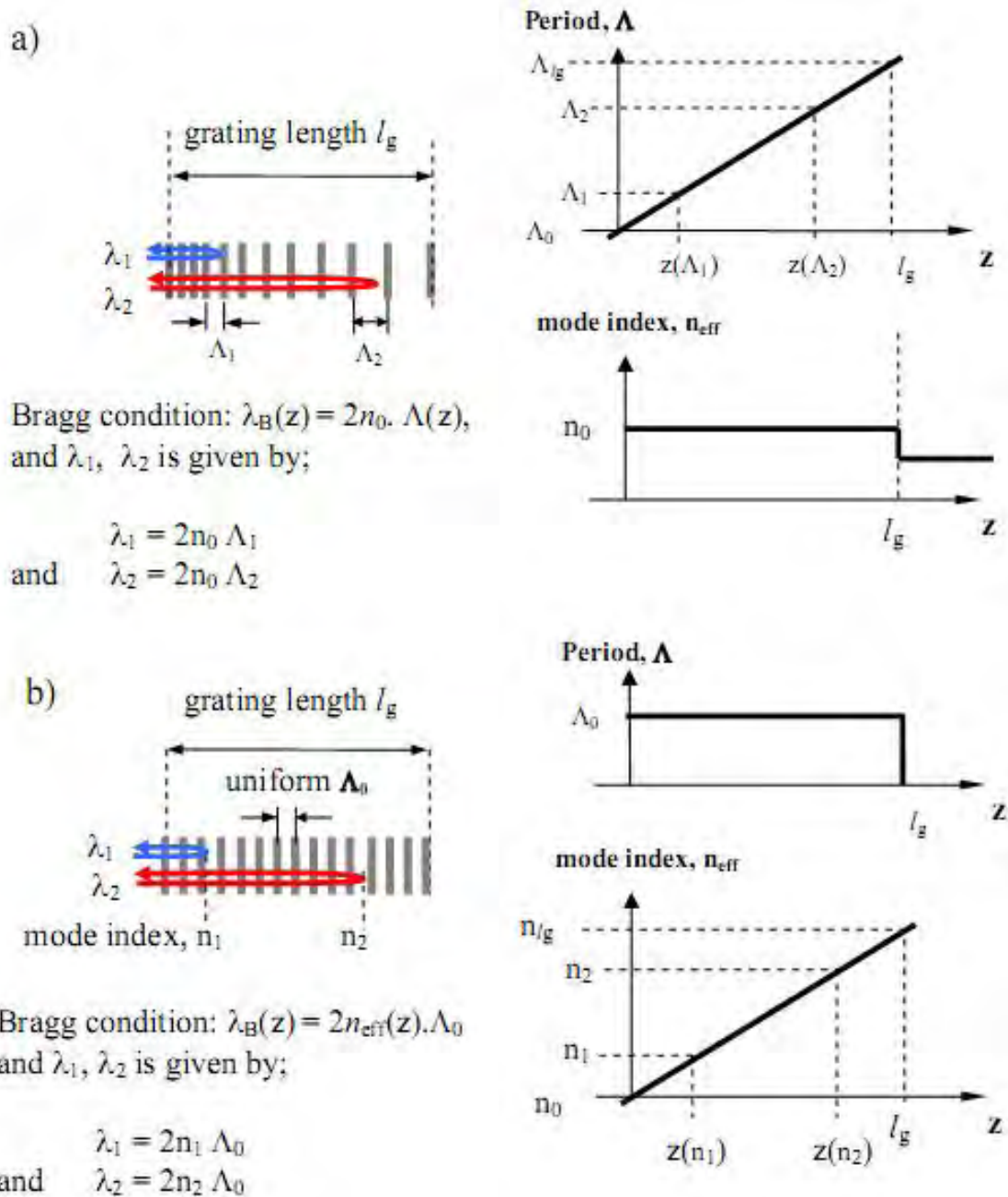


Fig. 2.3 Illustration of the chirped FBG with position detuned Bragg wavelength where the detuning is, a) driven by the position dependence periodicity, $\Lambda(z)$ and b) is driven by the varying mode index with position $n_{eff}(z)$.

2.2.3 Apodized FBG

There are basically two quantities that control the properties of the FBG. These are the grating length, L_g and the grating strength. Grating length is given by

$$L_g = NA \quad (2.5)$$

and the grating strength, n_{eff} . There are, however, three properties that need to be controlled in a FBG. These are the reflectivity, the bandwidth, and the side-lobe strength. As shown above, the bandwidth depends on the grating strength, and not the grating length. This means the grating strength can be used to set the bandwidth. The grating length, effectively L , can then be used to set the peak reflectivity, which depends on both the grating strength and the grating length. The result of this is that the side lobe strength cannot be controlled, and this simple optimization results in significant side lobes. A third quantity can be varied to help with side-lobe suppression. This is apodization of the refractive index change.

Fiber gratings are not infinite in length, so they have a beginning and an end. Thus, they begin abruptly and end abruptly. The Fourier transform of such a “rectangular” function immediately yields the well known *sinc* function, with its associated side-lobe structure apparent in the reflection spectrum. The transform of a Gaussian function, for example, is also a Gaussian, with no side lobes. A grating with similar refractive modulation amplitude profile diminishes the side lobes substantially. The suppression of the side lobes in the reflection spectrum by gradually increasing the coupling coefficient with penetration into, as well as gradually decreasing on exiting from, the grating is called apodization. The term apodization refers to the grading of the refractive index to approach zero at the end of the grating. K. O. Hill [15] showed that apodization of a periodic waveguide structure suppresses the side lobes.

Apodized gratings offer significant improvement in side-lobe suppression while maintaining reflectivity and a narrow bandwidth.

2.2.4 Tilted Fiber Bragg Gratings

In standard FBGs, the grading or variation of the refractive index is along the length of the fiber (the optical axis), and is typically uniform across the width of the fiber. In a tilted FBG (TFBG), the variation of the refractive index is at an angle to the optical axis. The angle of tilt in a TFBG has an effect on the reflected wavelength, and bandwidth.

2.2.5 Long-period Gratings

Typically the grating period is the same size as the Bragg wavelength, as shown above. For a grating that reflects at 1500 nm, the grating period is 500 nm, using a refractive index of 1.5. Longer periods can be used to achieve much broader responses than are possible with a standard FBG. These gratings are called long-period fiber grating. They typically have grating periods on the order of 100 micrometers, to a millimeter, and are therefore much easier to manufacture.

2.3 Application of Fiber Bragg Gratings

Fiber Bragg grating technology develop rapidly after UV light side written technology was developed. Since then, much research has done to improve the quality and durability of fiber Bragg gratings. Fiber gratings are the keys to modern optical fiber communications and sensors. The commercial products of fiber Bragg gratings has been available since early 1995. Some common applications of fiber Bragg grating are listed below.

- Temperature, strain and pressure sensors.
- Distributed fiber Bragg grating sensors systems.
- Fiber grating semiconductor lasers.
- Stabilization of external cavity semiconductor lasers.
- Erbium-doped fiber lasers.
- Dispersion compensation.
- Wavelength division multiplexed networks.
- Gain flattening for erbium-doped fiber amplifiers.
- Add/Drop multiplexers.
- Comb filters.
- Interference reflectors.
- Pulse compressor.
- Wavelength tuning.
- Raman amplifiers.
- Chirped pulse amplification.

2.4 Dispersion in Single Mode Fiber

A singlemode fiber carries only one mode and therefore does not experience intermodal dispersion. Thus one would expect a singlemode fiber to have lower dispersion or, equivalently much higher bandwidth than a multimode fiber. However, pulse broadening does not disappear altogether. The group velocity associated with the fundamental mode is frequency dependent because of chromatic dispersion. As a result, different spectral components of the pulse travel at slightly different group velocities, a phenomenon referred to as group-velocity dispersion (GVD) or intramodal dispersion. The major mechanism that causes dispersion in a singlemode fiber is chromatic dispersion. Two mechanisms play an important role in chromatic dispersion are material dispersion and waveguide dispersion.

2.5 Chromatic Dispersion

Chromatic dispersion (CD) is the spreading of a light pulse as it travels down a fiber. Light has a dual nature and can be considered from an electromagnetic wave as well as a quantum perspective. This enables us to quantify it as waves as well as quantum particles. During the propagation of light, all of its spectral components propagate accordingly. These spectral components travel at different group velocities that lead to dispersion called group velocity dispersion (GVD). Dispersion resulting from GVD is termed chromatic dispersion due to its wavelength dependence. Light of different wavelengths travel along the fiber at different velocities. Even if all of the beams propagate along the same path, they will arrive at the receiver end at different times. This results in the spreading of the light pulse, which is called chromatic dispersion. The effect of chromatic dispersion is pulse spread.

When an electromagnetic wave interacts with bound electrons of a dielectric, the medium's response in general depends on the optical frequency. This property is referred to as chromatic dispersion. The chromatic dispersion parameter in a single mode fiber is the sum of the material and waveguide dispersions, so that

$$D(\lambda) = D_M(\lambda) + D_W(\lambda) \quad (2.7)$$

This relation is very important since the material dispersion parameter above 1300 nm becomes positive while the waveguide dispersion parameter stays negative. The fact is that they cancel each other out, resulting in a zero chromatic – dispersion parameter $D(\lambda) = 0$. This occur around 1310 nm, the customary operating wave for standard single mode fiber as shown in Fig. 2.4.

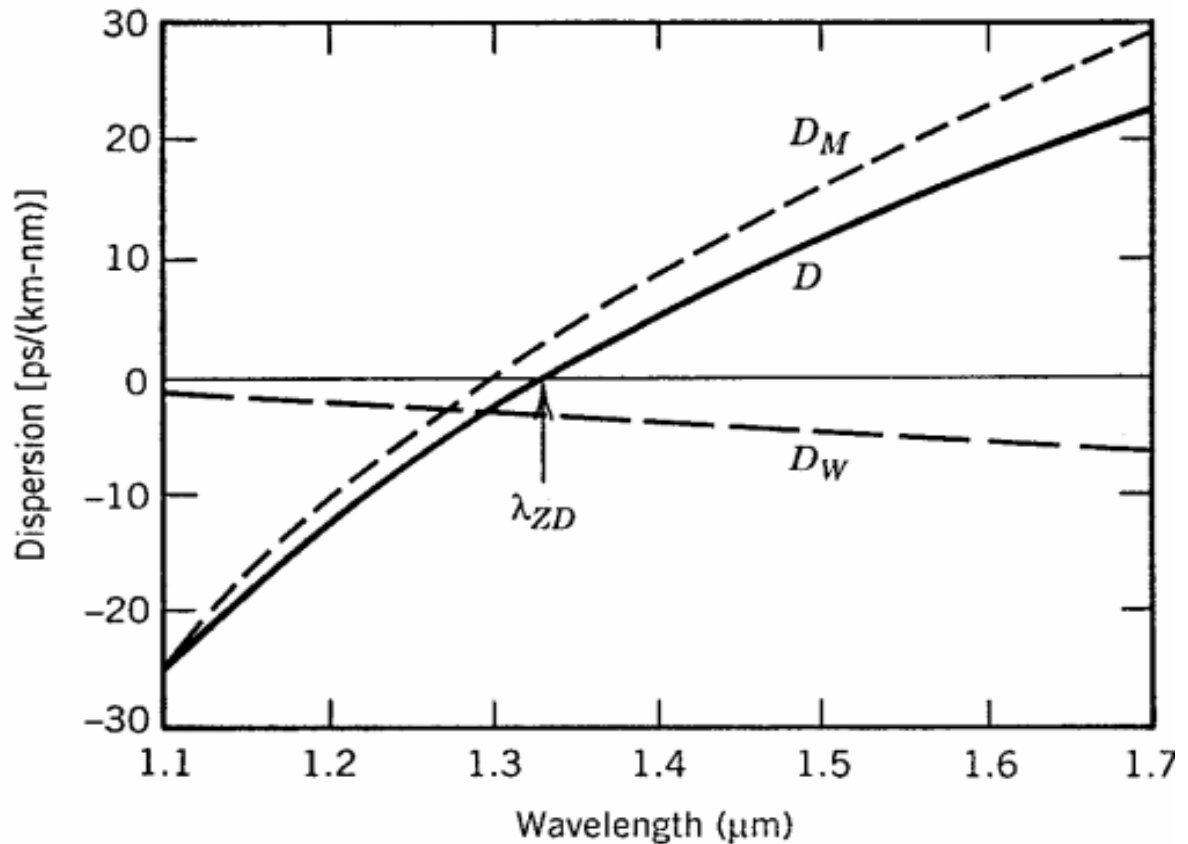


Fig. 2.4 Total dispersion D and relative contributions of material dispersion (MD) and waveguide dispersion (WD) for a conventional single-mode fiber.

Pulse spreading caused by chromatic dispersion,

$$\Delta t_{chrom} / L = D(\lambda)\Delta\lambda \quad (2.8)$$

,where $D(\lambda)$ is the chromatic dispersion parameter of the fiber and $\Delta\lambda$ is the spectral width of the light source. Manufacturers specify the CD parameter for fibers either by giving its value or by giving the formula.

$$D(\lambda) = \frac{S_0}{4} \left[\lambda - \frac{\lambda_0^4}{\lambda^3} \right] \quad (2.9)$$

,where S_0 is the zero-dispersion slope in ps/(nm².km), λ_0 is the zero dispersion wavelength, and λ is the operating wavelength.

To calculate the dispersion parameter near the zero dispersion wavelengths, λ_0 , one can use a simplified version of the above formula:

$$D(\lambda) = S_0[\lambda - \lambda_0] \quad (2.10)$$

,where the zero dispersion slope, S_0 can be found in a fiber data sheet.

The dispersion parameter D is commonly used in place of β_2 to describe the total dispersion of a single mode fiber. It is related to β_2 by the relation

$$D = \frac{d\beta_1}{d\lambda} = -\frac{2\pi c}{\lambda^2} \beta_2 \quad (2.11)$$

However, chromatic dispersion is an important phenomenon in the propagation of short pulses in optical fibers. Temporally short pulses have a large spectral bandwidth. The different spectral components of the pulse travel through the medium at slightly different group velocities because of chromatic dispersion, which can result in a temporal broadening of the light pulses with no effect on their spectral compositions.

2.6 Group Velocity Dispersion

Consider a single-mode fiber of length L . A specific spectral component at the frequency ω would arrive at the output end of the fiber after a time delay $T = L/v_g$, where v_g is the group velocity, defined as

$$v_g = \left(\frac{d\beta}{d\omega} \right)^{-1} \quad (2.12)$$

The frequency dependence of the group velocity leads to pulse broadening simply because different spectral components of the pulse disperse during propagation and do not arrive simultaneously at the fiber output. Group velocity dispersion (GVD) is an important effect because when a short pulse propagates through an optical fiber its pulse width gets broaden. The effects of fiber dispersion can be understood by expanding the mode- propagation

constant/phase constant β in a Taylor series about the frequency ω_0 at which the pulse spectrum is centered:

$$\beta(\omega) = n(\omega) \frac{\omega}{c} = \beta_0(\omega_0) + \frac{d\beta}{d\omega}(\omega - \omega_0) + \frac{1}{2} \frac{d^2\beta}{d\omega^2}(\omega - \omega_0)^2 + \frac{1}{6} \frac{d^3\beta}{d\omega^3}(\omega - \omega_0)^3 + \dots \quad (2.13)$$

,where, ω_0 is the centre frequency and β is frequency dependence, $\beta = f(\omega)$,

Here $\frac{d\beta}{d\omega} = \frac{1}{v_g} = \beta_1 = \text{Inverse group velocity} = \text{first - order dispersion}$.

Again, $\frac{d^2\beta}{d\omega^2} = \beta_2 = \text{First- order group velocity dispersion} = 2^{\text{nd}} \text{ order dispersion}$.

Again, $\frac{d^3\beta}{d\omega^3} = \beta_3 = \text{Second- order group velocity dispersion} = 3^{\text{rd}} \text{ order dispersion}$

$$\beta(\omega) = \beta_0(\omega_0) + \beta_1(\omega - \omega_0) + \frac{1}{2} \beta_2(\omega - \omega_0)^2 + \frac{1}{6} \beta_3(\omega - \omega_0)^3 + \dots \quad (2.14)$$

$$\text{,where } \beta_m = \left(\frac{d^m \beta}{d\omega^m} \right)_{\omega=\omega_0} \quad (m = 0, 1, 2, 3, \dots) \quad (2.15)$$

$$\beta_0 = n(\omega_0) \frac{\omega_0}{c} \quad (2.16)$$

$$\beta_1 = \frac{1}{c} \left(n + \omega \frac{dn}{d\omega} \right) = \frac{1}{v_g} = \frac{n_g}{c} \quad (2.17)$$

$$\beta_2 = \frac{1}{c} \left(2 \frac{dn}{d\omega} + \omega \frac{d^2n}{d\omega^2} \right) = \frac{d}{d\omega} \left(\frac{1}{v_g} \right) = -\frac{\lambda^2}{2\pi c} \cdot D \quad (2.18)$$

$$\begin{aligned} \beta_3 &= \frac{d^3\beta}{d\omega^3} = \frac{d}{d\omega} \left(\frac{d^2\beta}{d\omega^2} \right) = \frac{d\lambda}{d\omega} \cdot \frac{d}{d\lambda} \left(\frac{d^2\beta}{d\omega^2} \right) = \frac{d\lambda}{d\omega} \cdot \frac{d}{d\lambda} \left(-\frac{\lambda^2}{2\pi c} \cdot D \right) \\ &= \frac{1}{\lambda^2} \cdot \frac{-2\lambda}{2\pi c} \cdot \frac{d}{d\lambda} [\lambda^2 D] = \frac{\lambda^3}{2\pi^2 c^2} \left[D + \frac{\lambda}{2} \cdot \frac{dD}{d\lambda} \right] \end{aligned}$$

$$\therefore \beta_3 = \frac{\lambda^3}{2\pi^2 c^2} \left[\text{Dispersion} + \frac{\lambda}{2} \cdot \text{Dispersion_Slope} \right] \quad (2.19)$$

So, chromatic dispersion is define as

$$D_p = \frac{-2\pi c}{\lambda^2} \beta_2 \quad (2.20)$$

And dispersion slope is as,

$$dispersion_slope = \frac{dD_p}{d\lambda} \quad (2.21)$$

2.7 Summary

In this chapter basic concept of fiber Bragg grating and dispersion has been described. The applications of FBG also listed in this chapter. Chromatic dispersion and dispersion slope were illustrated, the group velocity dispersion also explained.

Chapter 3

Theoretical Analysis

3.1 Introduction

Fiber Bragg grating (FBG) is proving to be one of the most important developments in the field of the optical fiber technology [1]. With the rapid increase of information industry in the world, high speed and big capacity communication networks become more and more demandable. But dispersion becomes a major obstacle for up-gradation to this system. Apodized and linearly chirped fiber Bragg gratings (LCFBG) have proved to be an effective solution to compensate the chromatic dispersion of dense high bit-rate optical communication systems [2]. The availability of mass production techniques added to their inherent advantages, such as polarization insensitivity, fiber compatibility and the fact of being passive and low-loss devices make them very attractive over competing technologies [28]. As a first step, it is well known that an accurate modeling of the spectral behavior of the dispersion compensating fiber Bragg gratings can improve the efficiency of the design process, as well as the quality of the resulting devices.

3.2 System Model

In order to compare the effects of different apodization sharpness, we consider the system as shown in Fig. 3.1. The input pulses are launched to a link of standard single mode fiber. The output broadened pulses are then fed to a linearly chirped apodized grating through the optical circulator. This component also extracts the restored pulse that is reflected by the grating.

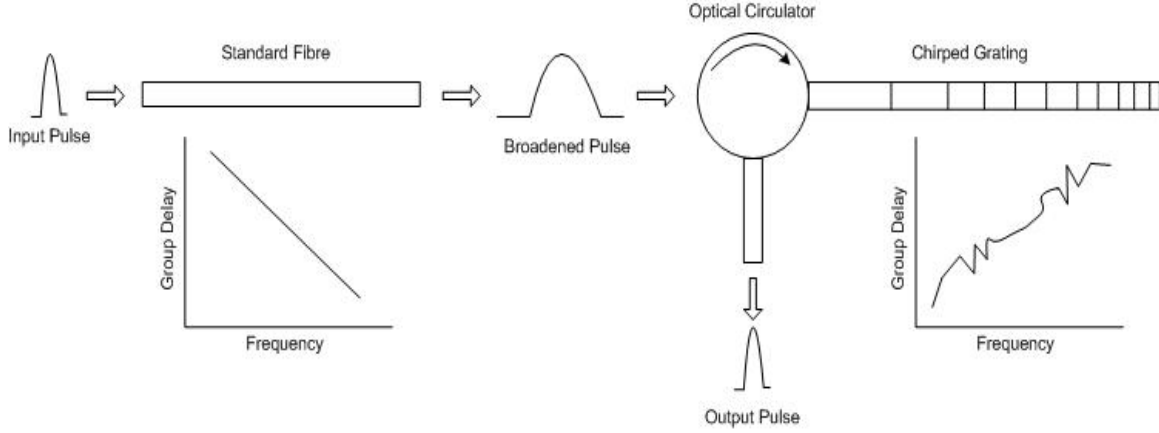


Fig. 3.1 System model of dispersion compensation

3.3 Pulse Broadening Factor in Dispersive Fiber

In a fiber optic communication system, information is transmitted over a fiber by using a coded sequence of optical pulses whose width is determined by the bit rate B of the system. Dispersion-induced broadening of pulses is undesirable as it interferes with the detection process and leads to errors if the pulse spread outside its allocated bit slot ($T_B = 1/B$). Clearly, dispersion limits the bit rate B for a fixed transmission distance L .

There are several methods that are used to measure the performance of an optical transmission system. But pulse broadening factor is a direct performance measure of the optical signal detection due to the optical fiber impairments.

The optical pulse propagation in a single mode fiber can be described by nonlinear Schrödinger equation (NLSE). This equation includes the effect of fiber losses, chromatic dispersion and fiber nonlinearity.

$$i \frac{\partial}{\partial z} A = -i \frac{\alpha}{2} A + \frac{\beta_2}{2} \frac{\partial^2}{\partial t^2} A + i \frac{\beta_3}{6} \frac{\partial^3}{\partial t^3} A - \gamma |A|^2 A \quad (3.1)$$

Where z is the longitudinal coordinate of the fiber, t is the time in a framework moving at the group velocity, A is the complex electrical field envelope, β_2 is the first order CD, β_3 is the second order CD, α is the power absorption coefficient, and γ is the nonlinear coefficient.

$$\gamma = \frac{2\pi n_2}{\lambda A_{eff}} \quad (3.2)$$

$$t = T - \frac{z}{v_g} \quad (3.3)$$

In order to access the effects of dispersion in the propagation of pulse we can neglect the effect of attenuation constant and nonlinear coefficient so (3.1) can be written as

$$i \frac{\partial}{\partial z} A = \frac{\beta_2}{2} \frac{\partial^2}{\partial t^2} A + i \frac{\beta_3}{6} \frac{\partial^3}{\partial t^3} A \quad (3.4)$$

Equation (3.4) can be solved by using the Fourier transform method if $\tilde{A}(z, \omega)$ is the Fourier transform of $A(z, t)$ such that

$$A(z, t) = \frac{1}{2\pi} \int_{-\infty}^{\infty} \tilde{A}(z, \omega) \exp(-i\omega t) d\omega \quad (3.5)$$

Differentiating equation (3.5) with respect to t

$$\frac{dA}{dt} = \frac{1}{2\pi} \tilde{A}(z, \omega) (-i\omega) \exp(-i\omega t) \quad (3.6)$$

$$\begin{aligned} \frac{d^2 A}{dt^2} &= \frac{1}{2\pi} \tilde{A}(z, \omega) (-i\omega)^2 \exp(-i\omega t) \\ &= \frac{-\exp(-i\omega t)}{2\pi} \tilde{A}(z, \omega) \omega^2 \end{aligned} \quad (3.7)$$

$$\begin{aligned} \frac{d^3 A}{dt^3} &= \frac{1}{2\pi} \tilde{A}(z, \omega) (-i\omega)^3 \exp(-i\omega t) \\ &= \frac{-i \exp(-i\omega t)}{2\pi} \tilde{A}(z, \omega) \omega^3 \end{aligned} \quad (3.8)$$

Differentiating equation (3.5) with respect to z

$$\frac{dA}{dz} = \frac{1}{2\pi} \tilde{A}(z, \omega) \exp(-i\omega t) \quad (3.9)$$

Putting these values in equation (3.4) can be obtained

$$\begin{aligned} \frac{\exp(-i\omega t)}{2\pi} i \frac{d}{dz} \tilde{A} &= -\frac{\beta_2}{2} \frac{-\exp(-i\omega t)}{2\pi} \tilde{A} \omega^2 + i \frac{\beta_3}{6} \frac{-i \exp(-i\omega t)}{2\pi} \tilde{A} \omega^3 \\ i \frac{d}{dz} \tilde{A} &= -\frac{\beta_2}{2} \tilde{A} \omega^2 - \frac{\beta_3}{6} \tilde{A} \omega^3 \\ i \frac{d \tilde{A}}{dz} + \left(\frac{\beta_2}{2} \omega^2 + \frac{\beta_3}{6} \omega^3 \right) \tilde{A} &= 0 \end{aligned} \quad (3.10)$$

Solution of this equation is given by

$$\tilde{A}(z, \omega) = \tilde{A}(0, \omega) \exp\left(\frac{\beta_2}{2} \omega^2 + \frac{\beta_3}{6} \omega^3\right) iz \quad (3.11)$$

Substituting equation (3.11) in equation (3.5) can be obtained

$$A(z, t) = \frac{1}{2\pi} \int_{-\infty}^{\infty} \tilde{A}(0, \omega) \exp\left[\left(\frac{\beta_2}{2} \omega^2 + \frac{\beta_3}{6} \omega^3\right) iz - i\omega t\right] d\omega \quad (3.12)$$

Where $\tilde{A}(0, \omega)$ is the Fourier transform of the incident field at $z = 0$ and is obtained by

$$\bar{A}(0, \omega) = \int_{-\infty}^{\infty} A(0, t) \exp(-i\omega t) dt \quad (3.13)$$

Eq. (3.12) can be used to obtain analytical expression for the output pulse; the RMS pulse width at a distance z is defined as

$$\Delta t(z) = \left[\langle t^2 \rangle - \langle t \rangle^2 \right]^{1/2} \quad (3.14)$$

,where

$$\langle t^n \rangle = \frac{\int_{-\infty}^{\infty} t^n |A(z, t)|^2 dt}{\int_{-\infty}^{\infty} |A(z, t)|^2 dt} \quad (3.15)$$

is the n^{th} moment. To evaluate the effects of β_2 and β_3 on pulse propagation by considering a Gaussian input pulse whose profile is defined as

$$A(0, t) = A_0 \exp\left(-\frac{t^2}{2T_0^2}\right) \quad (3.16)$$

Where, A_0 is the peak amplitude. The parameter T_0 is the half-width at $1/e$ intensity point and related to the full width at half maximum (FWHM) of the pulse by the relation

$$T_{FWHM} = 2\sqrt{2 \ln 2} T_0 \quad (3.17)$$

the spectrum of the input pulse is obtained by using the Fourier transform of $A(0, t)$

which is

$$\bar{A}(0, \omega) = \int_{-\infty}^{\infty} A(0, t) \exp(i\omega t) dt \quad (3.18)$$

Substituting equation (3.16) in equation (3.18) can obtained

$$A(0, \omega) = \int_{-\infty}^{\infty} A_0 \exp\left(-\frac{t^2}{2T_0^2}\right) \exp(-i\omega t) dt \quad (3.19)$$

By integrating equation (3.19) is acquired

$$\tilde{A}(\omega, 0) = A_0 (2\pi T_0^2)^{1/2} \exp\left(-\frac{1}{2}\omega^2 T_0^2\right) \quad (3.20)$$

Substituting equation (3.20) in equation (3.12) is obtained

$$A(z, t) = \frac{1}{2\pi} \int_{-\infty}^{\infty} A_0 (2\pi T_0^2)^{1/2} \exp\left(-\frac{1}{2}\omega^2 T_0^2\right) \exp\left[i\left\{\left(\frac{\beta_2}{2}\omega^2 + \frac{\beta_3}{6}\omega^3\right)z - \omega t\right\}\right] d\omega \quad (3.21)$$

By integrating equation (3.21) and solving can achieved

$$A(z, t) = \frac{A_0}{\sqrt{Q(z)}} \exp\left[-\frac{1}{2Q(z)}\left(\frac{t}{T_0}\right)^2\right] \quad (3.22)$$

,where

$$Q(z) = \frac{T_0^2 - iz(\beta_2 + \beta_3)}{T_0^2} \quad (3.23)$$

Equation (3.23) shows that a Gaussian pulse remains Gaussian during propagation but its width and amplitude change by the factor $Q(z)$.

Equation (3.22) can be written as

$$A(z, t) = \frac{A_0}{\sqrt{Q(z)}} h(z, t) \quad (3.24)$$

, where $h(z, t)$ is the output pulse shape at distance z and is defined as

$$h(z, t) = \exp\left[-\frac{1}{Q(z)}\left(\frac{t}{T_0}\right)^2\right] \quad (3.25)$$

Substituting equation (3.24) in (3.15)

$$\langle t^n \rangle = \frac{\int_{-\infty}^{\infty} t^n \left| \frac{A_0}{\sqrt{Q(z)}} h(z, t) \right|^2 dt}{\int_{-\infty}^{\infty} \left| \frac{A_0}{\sqrt{Q(z)}} h(z, t) \right|^2 dt}$$

$$\langle t^n \rangle = \frac{\int_{-\infty}^{\infty} t^n |h(z, t)|^2 dt}{\int_{-\infty}^{\infty} |h(z, t)|^2 dt} \quad (3.26)$$

$$|h(z, t)|^2 = |h(z, t)^* h(z, t)| \quad (3.27)$$

, where $h(z, t)^*$ is the complex conjugate of $h(z, t)$

$$|h(z, t)|^2 = \exp\left(-\frac{t^2 T_0^2}{T_0^4 + (\beta_2 + \beta_3)^2 z^2}\right) \quad (3.28)$$

$$\langle t^2 \rangle = \frac{\int_{-\infty}^{\infty} t^2 |h(z, t)|^2 dt}{\int_{-\infty}^{\infty} |h(z, t)|^2 dt} \quad (3.29)$$

Substituting (3.28) in (3.29)

$$\langle t^2 \rangle = \frac{\int_{-\infty}^{\infty} t^2 \left| \exp\left(-\frac{t^2 T_0^2}{T_0^4 + (\beta_2 + \beta_3)^2 z^2}\right) \right|^2 dt}{\int_{-\infty}^{\infty} \left| \exp\left(-\frac{t^2 T_0^2}{T_0^4 + (\beta_2 + \beta_3)^2 z^2}\right) \right|^2 dt} \quad (3.30)$$

$$\langle t^2 \rangle = \frac{T_0^4 + (\beta_2 + \beta_3)^2 z^2}{2T_0^2}$$

$$\langle t \rangle = \frac{\int_{-\infty}^{\infty} t \left| \exp\left(-\frac{t^2 T_0^2}{T_0^4 + (\beta_2 + \beta_3)^2 z^2}\right) \right|^2 dt}{\int_{-\infty}^{\infty} \left| \exp\left(-\frac{t^2 T_0^2}{T_0^4 + (\beta_2 + \beta_3)^2 z^2}\right) \right|^2 dt}$$

since

$$\int_{-\infty}^{\infty} t \exp\left(-\frac{t^2 T_0^2}{T_0^4 + (\beta_2 + \beta_3)^2 z^2}\right) dt = 0$$

because it is an odd function of t .

$$\langle t \rangle = \frac{\int_{-\infty}^{\infty} t \left| \exp\left(-\frac{t^2 T_0^2}{T_0^4 + (\beta_2 + \beta_3)^2 z^2}\right) \right|^2 dt}{\int_{-\infty}^{\infty} \left| \exp\left(-\frac{t^2 T_0^2}{T_0^4 + (\beta_2 + \beta_3)^2 z^2}\right) \right|^2 dt} = 0 \quad (3.31)$$

Substituting equations (3.30) and (3.31) in equation (3.14) and squaring both sides

$$\Delta t^2(z) = \frac{T_0^4 + (\beta_2 + \beta_3)^2 z^2}{2T_0^2} \quad (3.32)$$

The input root mean square (RMS) pulse width is defined as

$$\Delta t_0 = \frac{T_0}{\sqrt{2}} \quad (3.33)$$

$$\Delta t_0^2 = \frac{T_0^2}{2}$$

$$\frac{\Delta t^2(z)}{\Delta t_0^2} = \frac{T_0^4 + (\beta_2 + \beta_3)^2 z^2}{T_0^4} \quad (3.34)$$

Pulse broadening factor which is the final to the initial RMS pulse width ratio is defined as

$$\hat{U} = \left| \frac{\Delta t^2(z)}{\Delta t_0^2} \right|^{1/2} = \left(\frac{T_0^4 + (\beta_2 + \beta_3)^2 z^2}{T_0^4} \right)^{1/2} \quad (3.35)$$

Equation (3.35) describes the pulse broadening factor in a linear dispersive fiber.

3.4 Phase of Reflectivity and Time Delay of FBG

The most widely used theory of fiber gratings is the coupled-mode theory because the theory is a good tool for obtaining quantitative information about the diffraction efficiency and spectral dependence of fiber gratings. The coupled-mode theory is used to determine the phase of reflectivity and delay introduced by the FBG. The main spectral

function under the study is the reflection coefficient, $r = |\rho|^2$ where ρ is the reflectivity coefficient can be written as following.

$$\rho = \frac{-\kappa \sinh(\sqrt{\gamma L_g})}{\hat{\sigma} \sinh(\sqrt{\gamma L_g}) + i\gamma \cosh(\sqrt{\gamma L_g})} \quad (3.36)$$

,where $\gamma = \kappa^2 - \hat{\sigma}^2$

$\hat{\sigma}$ = general ‘dc’ self coupling coefficient define as

$\hat{\sigma} = \delta + \sigma - \frac{1}{2} \frac{d\varphi}{dz}$; where $\frac{d\varphi}{dz}$ possible chirped of grating period

σ =”dc” coupling coefficient define as

$$\sigma = \frac{2\pi}{\lambda} \Delta n$$

Δn = modulation index change spatially averaged over a grating period.

δ = detuning which is independent of z for all gratings is define as

$$\delta = \beta - \frac{\pi}{\Lambda} = \frac{2\pi n_{eff}}{\lambda} - \frac{2\pi n_{eff}}{\lambda_B} = \frac{n_{eff}}{c} \left(\frac{2\pi c}{\lambda} - \frac{2\pi c}{\lambda_B} \right)$$

$$\delta = \frac{n_{eff}}{c} (\omega - \omega_B)$$

Hence, δ is the detuning of the channel carrier frequency ω from the resonant Bragg frequency ω_B .

κ = “ac” coupling coefficient defines as

$$\kappa(z) = \frac{\pi}{\lambda_B} \frac{\Delta n}{n_{eff}} T(z)$$

where $T(z)$ is the apodization function.

To get the phase of the reflectivity, it is needed to separate the real and imaginary parts from equation (3.36),

$$\rho = \frac{-\kappa \sinh(\sqrt{\gamma L_g}) \left\{ \hat{\sigma} \sinh(\sqrt{\gamma L_g}) - i\gamma \cosh(\sqrt{\gamma L_g}) \right\}}{\hat{\sigma}^2 \sinh^2(\gamma L_g) + \gamma^2 \cosh^2(\gamma L_g)} \quad (3.37)$$

$$\rho = -\frac{\kappa \hat{\sigma} \sinh(\sqrt{\gamma L_g}) \sinh(\sqrt{\gamma L_g})}{\hat{\sigma}^2 \sinh^2(\gamma L_g) + \gamma^2 \cosh^2(\gamma L_g)} + i \frac{\kappa \gamma \sinh(\sqrt{\gamma L_g}) \cosh(\sqrt{\gamma L_g})}{\hat{\sigma}^2 \sinh^2(\gamma L_g) + \gamma^2 \cosh^2(\gamma L_g)} \quad (3.38)$$

From equation (3.38), the phase of the reflectivity is found and is given in equation (3.39)

$$\begin{aligned} \therefore \angle \rho = \theta_p &= -\tan^{-1} \frac{\gamma \cosh(\sqrt{\gamma L_g})}{\hat{\sigma} \sinh(\sqrt{\gamma L_g})} \\ \theta_p &= -\tan^{-1} \left(\frac{\gamma}{\sqrt{\kappa^2 - \gamma^2}} \coth(\sqrt{\gamma L_g}) \right) \end{aligned} \quad (3.39)$$

The delay time τ_p for light reflected off a grating is [3]

$$\tau_p = \frac{d\theta_p}{d\omega} = -\frac{\lambda^2}{2\pi c} \frac{d\theta_p}{d\lambda} \quad (3.40)$$

$$\tau_p = -\frac{\lambda^2}{2\pi c} \frac{d\theta_p}{d\gamma} \frac{d\gamma}{d\hat{\sigma}} \frac{d\hat{\sigma}}{d\lambda} \quad (3.41)$$

Different parts of equation (3.41) can be differentiate as follows

$$\frac{d\theta_p}{d\gamma} = \frac{d}{d\gamma} \left[-\tan^{-1} \left(\frac{\gamma}{\sqrt{\kappa^2 - \gamma^2}} \coth(\gamma L_g) \right) \right] \quad (3.42)$$

$$\frac{d\gamma}{d\hat{\sigma}} = \frac{d}{d\hat{\sigma}} \left(\sqrt{\kappa^2 - \hat{\sigma}^2} \right) \quad (3.43)$$

$$\frac{d\hat{\sigma}}{d\lambda} = \frac{d}{d\lambda} \left(\delta + \sigma - \frac{1}{2} \right) \quad (3.44)$$

By solving the differentials equations (3.42), (3.43) and (3.44) and substitute the results in equation (3.41), the value of time delay τ_p is found as shown in the equation (3.45)

$$\tau_p = \frac{\hat{\sigma}^3 n_{eff}}{\{\hat{\sigma}^2 + \gamma^2 \coth(\gamma L_g)^2\} \sqrt{\gamma c}} \left(\frac{\coth(\gamma L_g)}{\hat{\sigma}} - \gamma \hat{\sigma}^{-3/2} \coth(\gamma L_g) - \frac{\gamma L_g \csc h^2(\gamma L_g)}{\hat{\sigma}} \right) \quad (3.45)$$

τ_p is usually given in units of picoseconds. The second order dispersion D_p (in ps/nm) is the rate of change of delay with respect to wavelength [28],

$$D_p = \frac{d\tau_p}{d\lambda} = -\frac{2\pi c}{\lambda^2} \frac{d^2\theta_p}{d\omega^2} \quad (3.46)$$

Third order or dispersion slope is calculated as rate of change of D_p with respect to $d\lambda$, that is

$$\frac{d}{d\lambda} (D_p) = \frac{d}{d\lambda} \left(\frac{d\tau_p}{d\lambda} \right) = \frac{d}{d\lambda} \left(-\frac{2\pi c}{\lambda^2} \frac{d^2\theta_p}{d\omega^2} \right) \quad (3.47)$$

3.5 Analytical Formulation for Dispersion

The effect of dispersion can be understood by expanding mode propagation constant β in a Taylor series about ω .

$$\beta(\omega) = \beta_0(\omega_0) + \frac{d\beta}{d\omega}(\omega - \omega_0) + \frac{1}{2} \frac{d^2\beta}{d\omega^2}(\omega - \omega_0)^2 + \frac{1}{6} \frac{d^3\beta}{d\omega^3}(\omega - \omega_0)^3 + \dots \quad (3.48)$$

So the m^{th} order dispersion coefficient of the grating β_m can be approximated as

$$\beta_m = \left. \frac{d^m \beta}{d\omega^m} \right|_{\omega=\omega_0} \quad (3.49)$$

as we know, $\delta = \frac{n_{\text{eff}}}{c}(\omega - \omega_B)$

Now the effect of the grating dispersion can be accounted for mathematically by expanding propagation constant β in a Taylor series about δ .

$$\beta(\delta) = \beta_0(\delta_0) + \frac{c}{n_{\text{eff}}} \frac{d\beta}{d\delta}(\delta - \delta_0) + \frac{1}{2} \left(\frac{c}{n_{\text{eff}}} \right)^2 \frac{d^2\beta}{d\delta^2}(\delta - \delta_0)^2 + \frac{1}{6} \left(\frac{c}{n_{\text{eff}}} \right)^3 \frac{d^3\beta}{d\delta^3}(\delta - \delta_0)^3 + \dots \quad (3.50)$$

So the m^{th} order dispersion coefficient of the grating β_m where $m=1,2,3,\dots$ can be approximated as

$$\beta_m = \left(\frac{c}{n_{\text{eff}}} \right)^m \left. \frac{d^m \beta}{d\delta^m} \right|_{\delta=\delta_0} \quad (3.51)$$

The propagation constant relation is given by

$$\beta = \pm \sqrt{\delta^2 - \kappa^2} \quad (3.52)$$

This is showing the relation among the frequency detuning parameter δ ; the coupling coefficient κ and propagation constant β .

Differentiating equation (3.52) with respect to δ and thus equation (3.53) is derived; the term β_1 is inverse group velocity.

$$\begin{aligned}\frac{d\beta}{d\delta} &= \frac{d}{d\delta} \left(\sqrt{\delta^2 - \kappa^2} \right) \\ \frac{d\beta}{d\delta} &= \beta_1 = \frac{\delta}{\sqrt{\delta^2 - \kappa^2}}\end{aligned}\quad (3.53)$$

The term β_2 is the first order group velocity dispersion can be derived as follows

$$\begin{aligned}\frac{d^2\beta}{d\delta^2} &= \frac{d\beta_1}{d\delta} = \frac{d}{d\delta} \left(\frac{\delta}{\sqrt{\delta^2 - \kappa^2}} \right) \\ \beta_2 &= \frac{-\kappa^2}{(\delta^2 - \kappa^2)^{3/2}}\end{aligned}\quad (3.54)$$

and β_3 is the second order group velocity dispersion can be derived by differentiating β_2 again

$$\begin{aligned}\frac{d^3\beta}{d\delta^3} &= \frac{d\beta_2}{d\delta} = \frac{d}{d\delta} \left[\frac{-\kappa^2}{(\delta^2 - \kappa^2)^{3/2}} \right] \\ \beta_3 &= \frac{3\kappa^2\delta}{(\delta^2 - \kappa^2)^{5/2}}\end{aligned}\quad (3.55)$$

The coupling coefficient κ , is given by equation (3.49) as follows

$$\kappa = \frac{\pi\Delta n}{\lambda_B n_{eff}} T(z), \text{ as } \lambda_B = 2n_{eff}\Lambda \text{ so } \kappa \text{ can be written as equation (3.68)}$$

$$\kappa = \frac{\pi\Delta n}{2n_{eff}^2\Lambda} T(z) \quad (3.56)$$

where, Λ is the grating period and $T(z)$ is the apodization function.

By substituting the value of equation (3.56) in equation (3.54) the second order dispersion can be obtained

$$\beta_2 = \frac{-2n_{eff}\Lambda [\pi\Delta n T(z)]^2}{\left[\{2\delta n_{eff}\Lambda T(z)\}^2 - \{\pi\Delta n T(z)\}^2 \right]^{3/2}} \quad (3.57)$$

By putting the value of equation (3.56) in equation (3.55) the third order dispersion can be derived as shown in equation (3.58).

$$\beta_3 = \frac{3\delta \{ \pi \delta n_{eff} T(z) \}^2 (2n_{eff}^2 \Lambda)^{3/2}}{\left[(\delta 2n_{eff} \Lambda)^2 - \{ \pi \Delta n T(z) \}^2 \right]^{3/2}} \quad (3.58)$$

So, chromatic dispersion is define as in equation (2.23) $D_p = \frac{-2\pi c}{\lambda^2} \beta_2$, hence equation (3.59) is obtained for chromatic dispersion.

$$D_p = \frac{4\pi c n_{eff} \Lambda \left[\pi \Delta n T(z) \right]^2}{\lambda^2 \left[\{ 2\delta n_{eff} \Lambda T(z) \}^2 - \{ \pi \Delta n T(z) \}^2 \right]^{3/2}} \quad (3.59)$$

And dispersion slope is given as in equation (2.24), $dispersion_slope = \frac{dD_p}{d\lambda}$, hence equation (3.60) can be derived as dispersion slope equation.

$$dispersion_slope = \frac{dD_p}{d\lambda} = 1 - \frac{4\pi c n_{eff} \Lambda \left[\pi \Delta n T(z) \right]^2}{\lambda} \quad (3.60)$$

3.6 Apodization Profiles

It is well known that the apodized and linearly chirped Bragg gratings reduced the side lobe level in the reflectivity response and also the group delay response ripple. However, the different apodization profiles have the different impact; it would be very useful to investigate and to analyze the different functions to find out the most suitable one for dispersion compensation.

Here, we are considering the following six apodization profiles. All profiles are symmetric around the centre of the grating and normalized so that $T(0)=1$.

The ‘*tanh*’ profile is given in equation (3.61).

$$T(z) = 1 + \tanh \left[\beta \left(1 - 2 \left(\frac{z}{L_g} \right)^\alpha \right) \right] \quad (3.61)$$

The ‘hamming’ profile is given in equation (3.62).

$$T(z) = \frac{1 + H \cos \left(\frac{2\lambda z}{L_g} \right)}{1 + H} \quad (3.62)$$

The ‘Gauss’ profile is given in equation (3.63).

$$T(z) = \exp \left[-G \left(\frac{z}{L_g} \right)^2 \right] \quad (3.63)$$

The ‘cosine’ profile is given in equation (3.64).

$$T(z) = \cos^A \left(\frac{\Pi}{L_g} z \right) \quad (3.64)$$

The ‘Cauchy’ profile is given in equation (3.65).

$$T(z) = \frac{1 - \left(\frac{2z}{L_g} \right)^2}{1 - \left(\frac{2Bz}{L_g} \right)^2} \quad (3.65)$$

The ‘sinc’ profile is given in equation (3.66).

$$T(z) = \operatorname{sinc}^X \left(\frac{\left| 2 \left(z - \frac{L_g}{2} \right) \right|^Y}{L_g} \right) \quad (3.66)$$

The parameter α , β , H , G , A , B , X and Y are used to control the apodization sharpness factor a_{eff} . The optimization process has been developed using the range of variation of these parameters to acquire a series of different apodization strengths by comparing the results obtained and applying each of the profiles to the dispersion compensating gratings.

The parameter that measures the strength of the apodization profile, and consequently the reduction of the effective length, is the apodization sharpness factor a_{eff} [5],

$$a_{eff} = \frac{\int_0^{L_g} |z| T(z) dz}{\int_0^{L_g} |z| dz} \quad (3.67)$$

Where L_g is the grating length, z is the position along the grating, $T(z)$ is the apodization profile.. The greater the apodization sharpness factor a_{eff} is, the tighter or sharper the apodization profile is. For unapodized gratings, $a_{eff}=1$.

3.7 Design Consideration of Linearly Chirped Grating Period

To reflect different wavelength at different time with the FBG, we need to chirp it. We introduce a linear chirp in the grating period by

$$\Lambda_N = M^{N-1} \Lambda_1 \quad (3.68)$$

where Λ_1 is the starting phase; M is the linear change of phase and N the number of grating period.

The total grating length L_g can be obtained by equation (3.69)

$$\begin{aligned} L_g &= \Lambda_1 + \Lambda_2 + \Lambda_3 + \dots + \Lambda_N \\ L_g &= \Lambda_1 + M \Lambda_1 + M^2 \Lambda_1 + \dots + M^{N-1} \Lambda_1 \\ L_g &= \sum_{N=0}^{N-1} M^N \Lambda_1 \end{aligned} \quad (3.69)$$

By Applying Geometric Series [12] the grating length L_g can be written as

$$L_g = \frac{\Lambda_1 (1 - M^N)}{1 - M} \quad (3.70)$$

3.8 Typical Optical Transmission System

Figure 3.2 shows generic block diagram of an optical communication system. It consists of a transmitter, a repeated unit of SMF, FBG and Erbium-Doped Fiber Amplifiers (EDFAs), and a receiver. The optical fiber is used as a medium to transmit the optical signals from the source to the destination. The input light pulses tend to spread while

traveling through the long optical fiber link, these phenomena is called chromatic dispersion (CD). In most of today's systems the accumulated pulse spreading caused by CD is compensated after each span by an FBG. FBG restores the broadened pulse and gives the output pulse identical to the input pulse. The optical fibers attenuate the signals during transmission, and therefore, it is required to use the optical amplifiers, such as, EDFAs to amplify the attenuated signal time to time, to restore the original signal level.

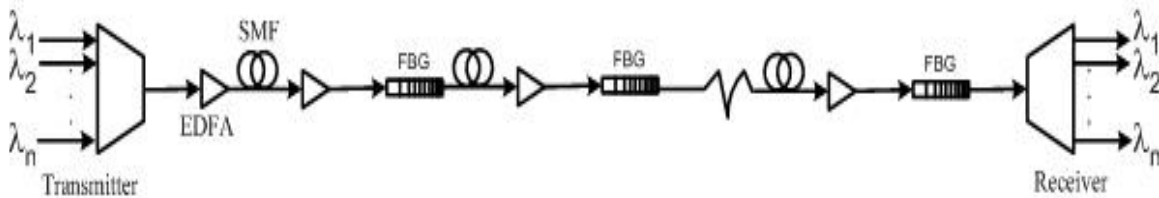


Fig. 3.2 A block diagram of an typical optical communication system.

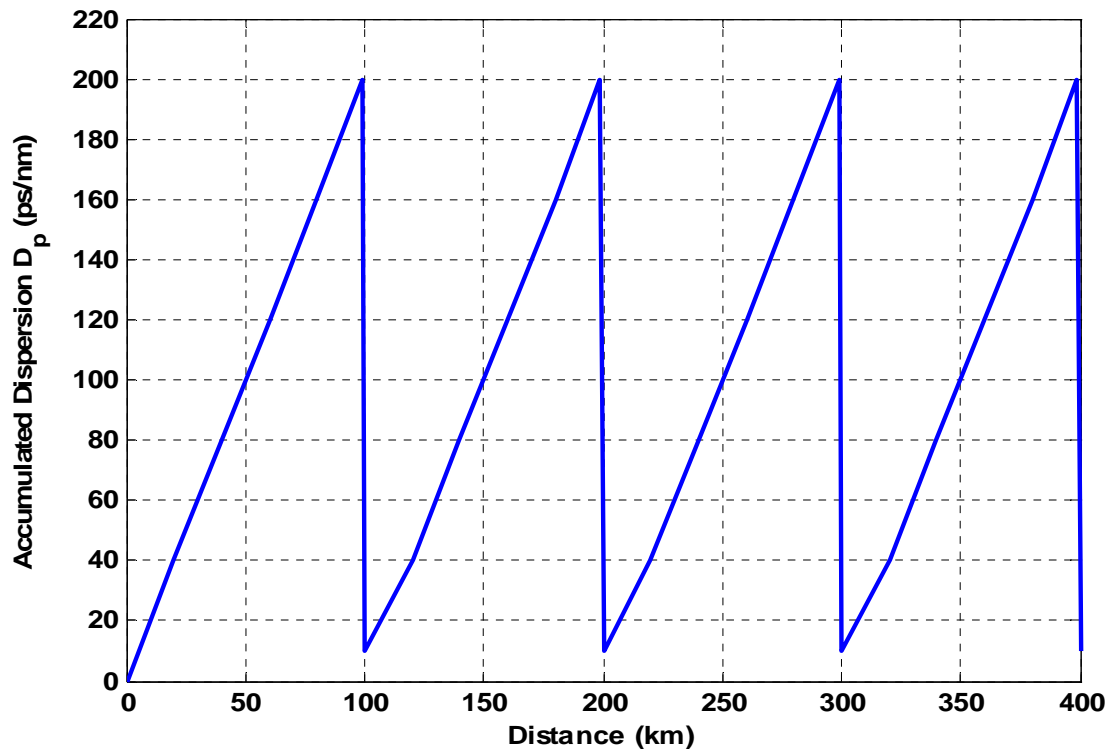


Fig. 3.3 Dispersion Compensation using FBG

Figure 3.3 show a dispersion compensation using FBG. From the figure it is found that dispersion increases as the signal travel more distance. If after every 100 km of fiber link

length a FBG is introduced in transmission system then the total dispersion trends to drop down near zero. This is shown in terms of initial, broadened and recompressed pulses in chapter 4.

3.9 Summary

In this chapter different analytical analysis has been carried out. At first pulse broadening factor in dispersive fiber is developed. Then phase of reflectivity and time delay of FBG has been formulated. Analytical model for dispersion relation, chromatic dispersion and dispersion slope is derived. Finally a model for linearly chirped grating period for FBG has been proposed. In the next chapter, all of the models will be simulated in the MATLAB environment and simulation results will be presented and discussed. Besides, proposed work will be compared with contemporary work.

Chapter 4

Results and Discussions

4.1 Introduction

This chapter explores the dispersion and dispersion slope compensation using different linearly chirped apodized fiber Bragg grating models through simulations. Pulse broadening effect for a Gaussian input pulse in dispersive fiber considering the effect of chromatic dispersion has been demonstrated. For simulation purpose, MATLAB software package is used. The set of parameter used to perform simulations are given in table 4.1

Table 4.1 Parameters used for simulation

Parameters	Settings
Central wavelength	1550 nm
Refractive index of the fiber core	1.46
Length of 1 st period	1.6 mm
Linearly decreasing factor	0.99 mm
No of segments	200
Grating Length	10 cm
Link length	100 km
Apodization profiles	<i>tanh</i> , hamming, Gauss, <i>cos</i> , <i>Cauchy</i> and <i>sinc</i>
Speed of light	3×10^8 m/sec
Data rate	10-40 Gb/s
Input power	30-120 mW
Fiber type	Standard single mode fiber

4.2 Determination of Appropriate Apodization Function

Following the mathematical formulation describe in chapter 3, we have plotted the optimization process for dispersion compensation. The effect of the apodization profiles on reflection spectra is investigated using six different profiles: *tanh*, hamming, gauss, *cos*, *Cauchy* and *sinc*. These are respectively displayed in Figs. 4.1-4.6.

Apodization is used to compensate sidelobe level in reflection spectrum but amplitude of the reflectivity will also need to consider. The apodization profile that shows a trade off between reflectivity and maximum suppression of sidelobe considered as the best profile, bandwidth is also considered. From Fig. 4.1 it is found that for *tanh* profile reflectivity is 98.55%, but it has significant sidelobe. $\Delta\lambda=0.2$ nm of bandwidth can be used from reflection spectrum. For hamming from the Fig. 4.2 it is observed that though the sidelobe is small but the reflectivity 97%. At the same time bandwidth is too small $\Delta\lambda<0.2$ nm. For Gauss reflectivity is 99% with a high sidelobe as shown in Fig. 4.3 bandwidth is also $\Delta\lambda<0.2$ nm. From Fig. 4.4 is found that for *cos* though bandwidth is bigger $\Delta\lambda>0.2$ nm and reflectivity is 99.98% but the sidelobe is very high. For *Cauchy* shown as Fig. 4.5 profile reflectivity is 88%, with reduce sidelobe and effective bandwidth is $\Delta\lambda<0.2$ nm. But *sinc* profile shows more than 96.95% reflectivity with minimum sidelobe and larger bandwidth $\Delta\lambda>0.2$ nm effective bandwidth. as shown in Fig. 4.5. So, *sinc* profile shows the superior performance with maximized both the reflectivity and reduction of sidelobe level among all profiles, for this case bandwidth is get a significant value.

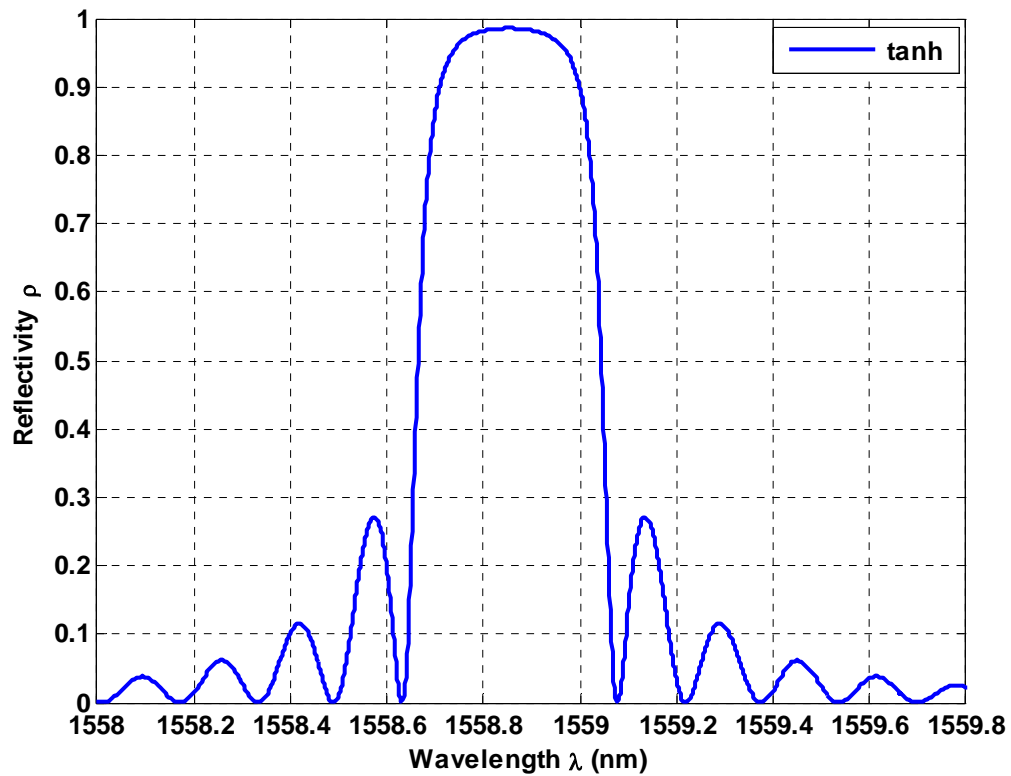


Fig. 4.1 Reflection spectrum of *tanh* profile for $\alpha=1$, $\beta=4$.

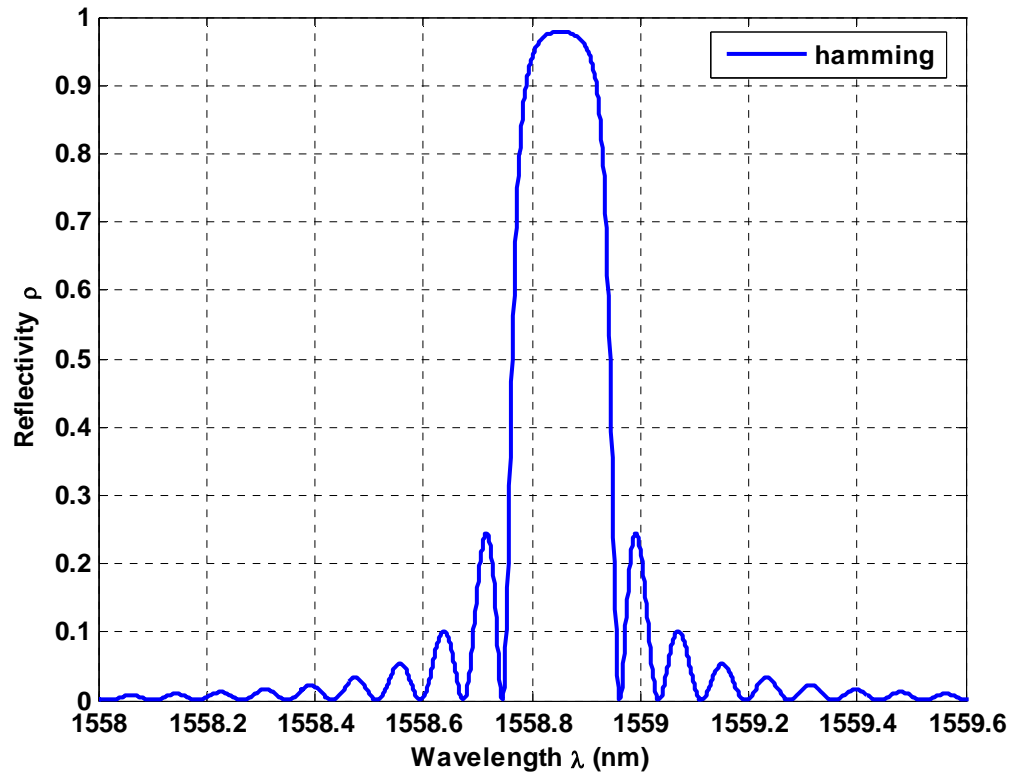


Fig. 4.2 Reflection spectrum of hamming profile for $H=0.8$.

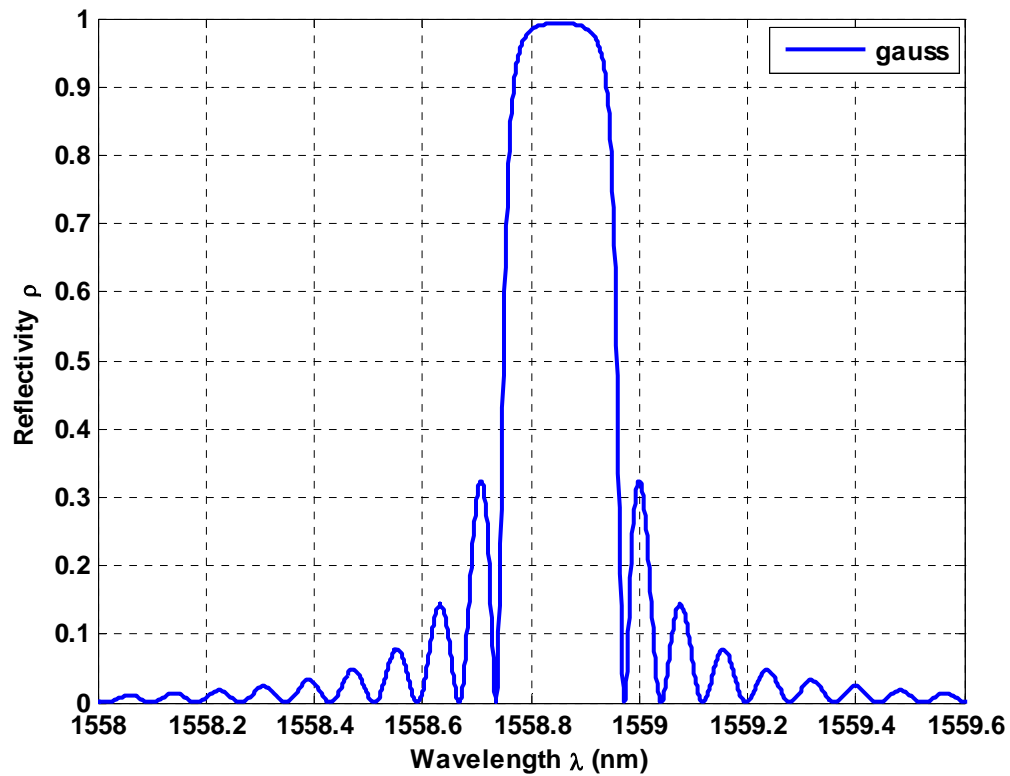


Fig. 4.3 Reflection spectrum of Gauss profile for $G=0.5$.

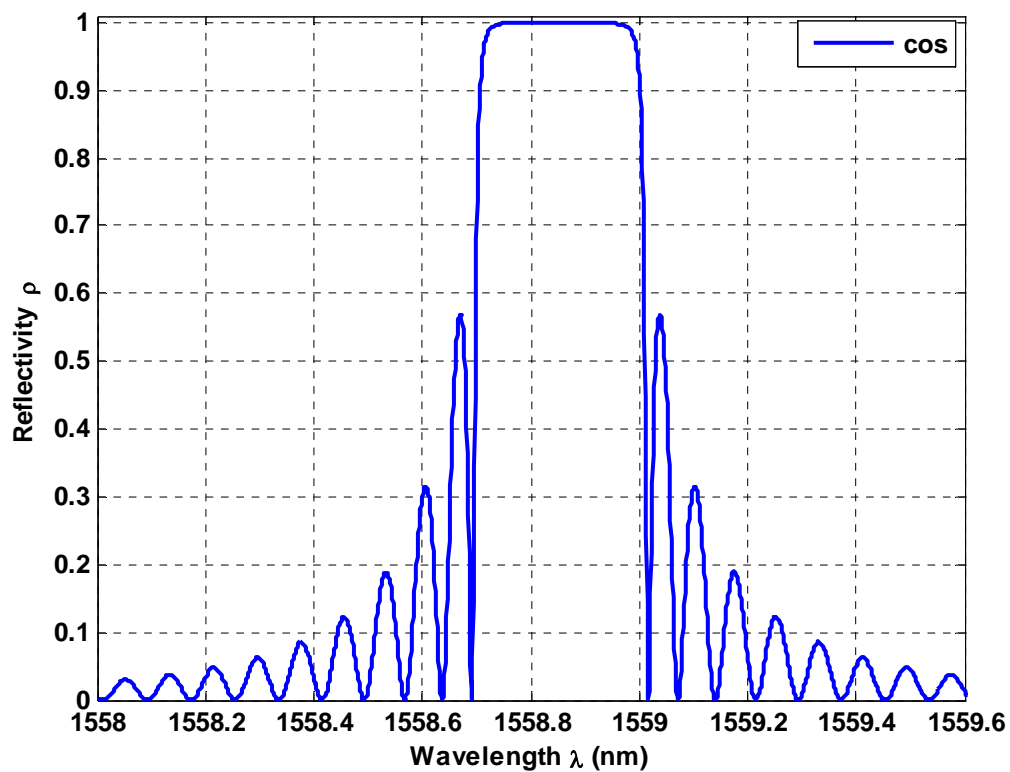


Fig. 4.4 Reflection spectrum of *cosine* profiles for $A=0.15$.

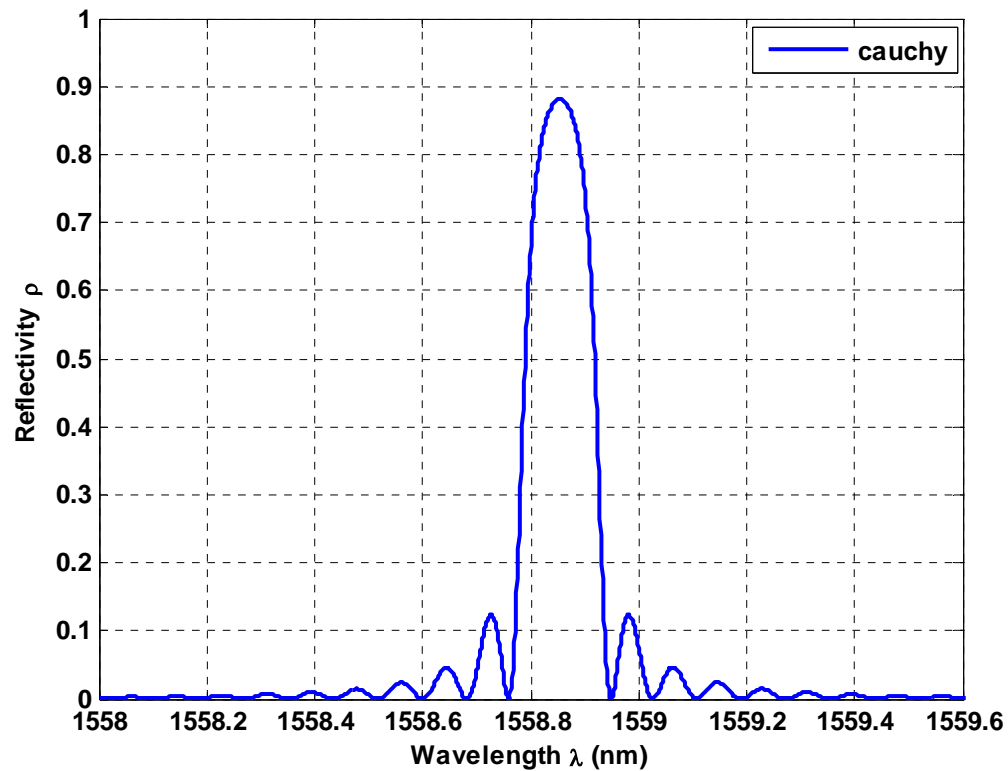


Fig. 4.5 Reflection spectrum of *Cauchy* profile for $B=0.2$.

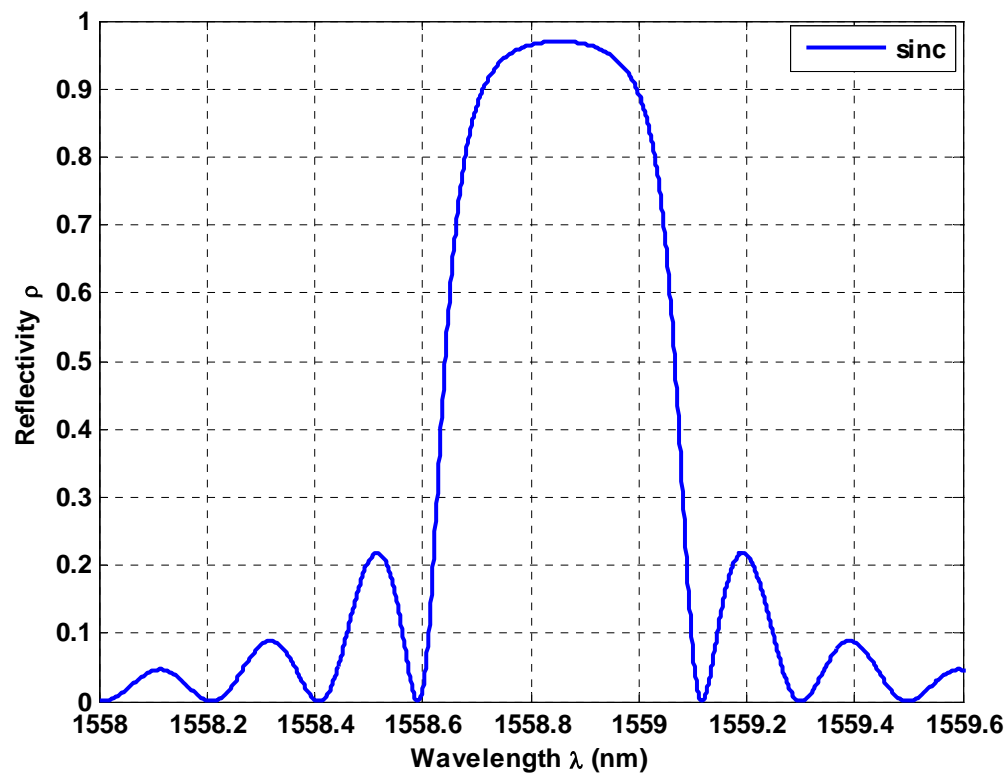


Fig. 4.6 Reflection spectrum of *sinc* profile for $X=1, Y=3$.

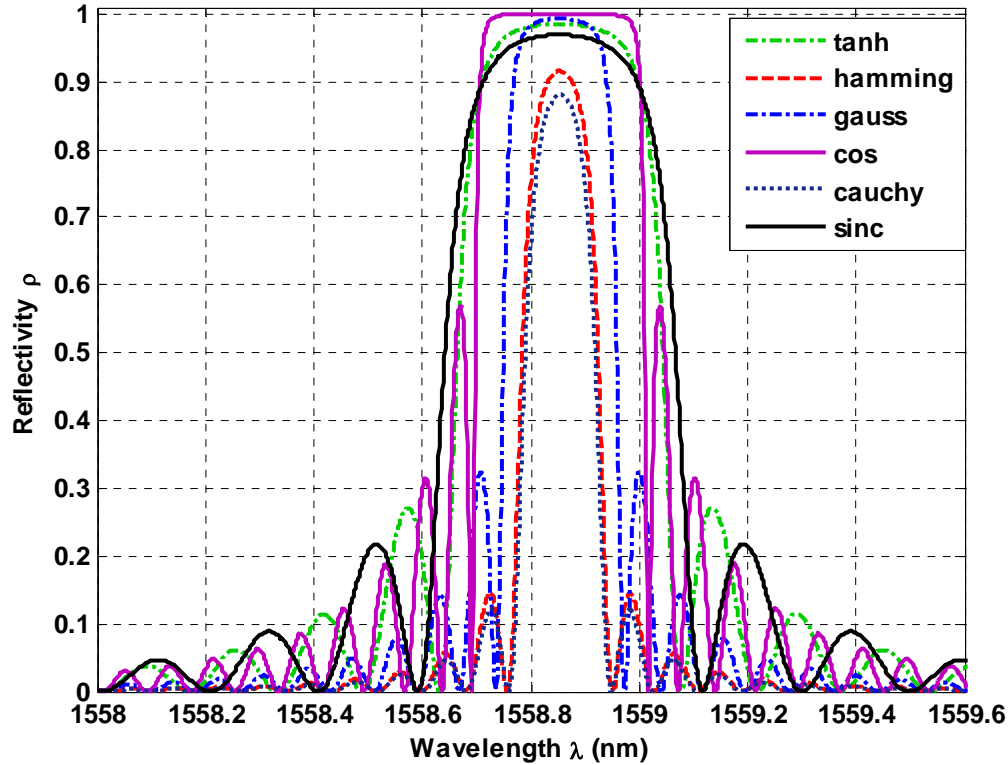


Fig. 4.7 Reflection spectrum of \tanh ($\alpha=1$, $\beta=4$), hamming ($H=0.8$), Gauss ($G=0.5$), cosine ($A=0.15$), Cauchy ($B=0.2$), sinc ($X=1$, $Y=3$) apodization profiles.

The parameter that measures the strength of the apodization profile, and consequently the reduction of the effective length, is the apodization factor a_{eff} . The greater the apodization factor a_{eff} is, the tighter or sharper the apodization profile is. So the largest possible values of a_{eff} are preferred. The parameter α , β , H , G , A , B , X and Y are used to control the apodization sharpness factor a_{eff} . The optimization process has been developed using the range of variation of these parameters, for ‘ \tanh ’ profile $\alpha \in [1, 4]$, $\beta \in [4, 8]$ for ‘hamming’ profile $H \in [0.1, 0.9]$, for ‘Gauss’ profile $G \in [0.5, 1.5]$, ‘cosine’ profile $A \in [0.15, 2]$, ‘Cauchy’ profile $B \in [0.2, 0.95]$ and for ‘sinc’ profile $X \in [1, 4]$, $Y \in [2, 6]$ to acquire a series of different apodization strengths by comparing the results obtained and applying each of the profiles to the dispersion compensating gratings.

Fig. 4.7 shows all super positioned reflection spectrum of \tanh ($\alpha=1$, $\beta=4$), hamming ($H=0.8$), Gauss ($G=0.5$), cosine ($A=0.15$), Cauchy ($B=0.2$), sinc ($X=1$, $Y=3$) apodization

profiles. These values for the parameter α , β , H , G , A , B , X and Y are used to get maximum apodization factor a_{eff} .

Grating length versus apodization strength for various apodization profiles have been investigated in Fig. 4.8 for 110 km of fiber length. It has been found that the grating length, $L_g = 10$ cm is sufficient for dispersion compensation. From Fig. 4.8 it has been found that for grating length 10 cm, apodization factor is the smallest 4.5 for hamming and 0.5 for *cos* profiles. For Cauchy it is about 0.52. And for Gauss profiles it is about 0.62. Apodization factor is 0.7 for *tanh* profile and for *sinc* profile it is more than 0.75, which is the largest value of a_{eff} among all profiles.

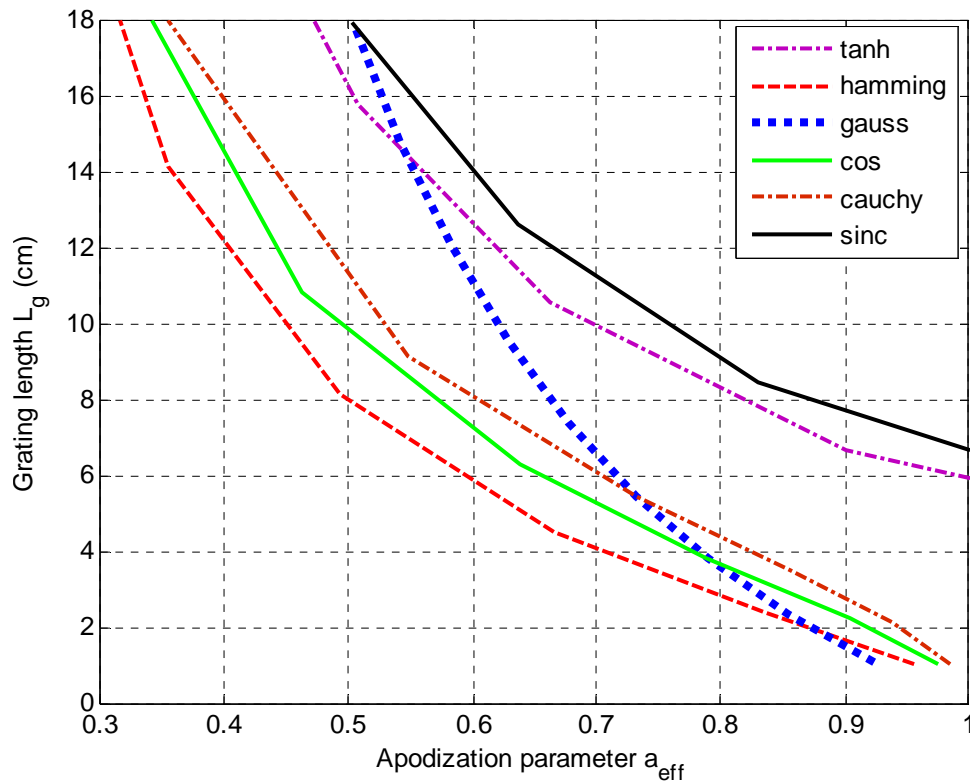


Fig. 4.8 Grating length versus apodization strength for *tanh* ($\alpha=1$, $\beta=4$), hamming ($H=0.8$), Gauss ($G=0.5$), cosine ($A=0.15$), Cauchy ($B=0.2$), *sinc* ($X=1$, $Y=3$) apodization profiles for 110 km of fiber length.

The values of the parameters which provide an efficient way to control the characteristics of the functions are chosen such that all the profiles have similar characteristics. An

important characteristic of apodization profile is a flat region at the grating centre and a constant slope decaying characteristics towards the grating edges. The effect of the apodization function versus normalized grating length is considered. The apodization functions provide these characteristics and they are represented in Fig. 4.9. Gauss and Hamming profiles provide a low decaying slope but with a reduced flat region at the grating's centre. In the case of the *tanh* function, the flat region is smaller and the slope at the decaying edges increases. *Cos* and *Cauchy* shows reduced flat region and slope at the decaying edge increases. In the last function, *sinc*, both the decaying slope and the flat region reach their maximum values.

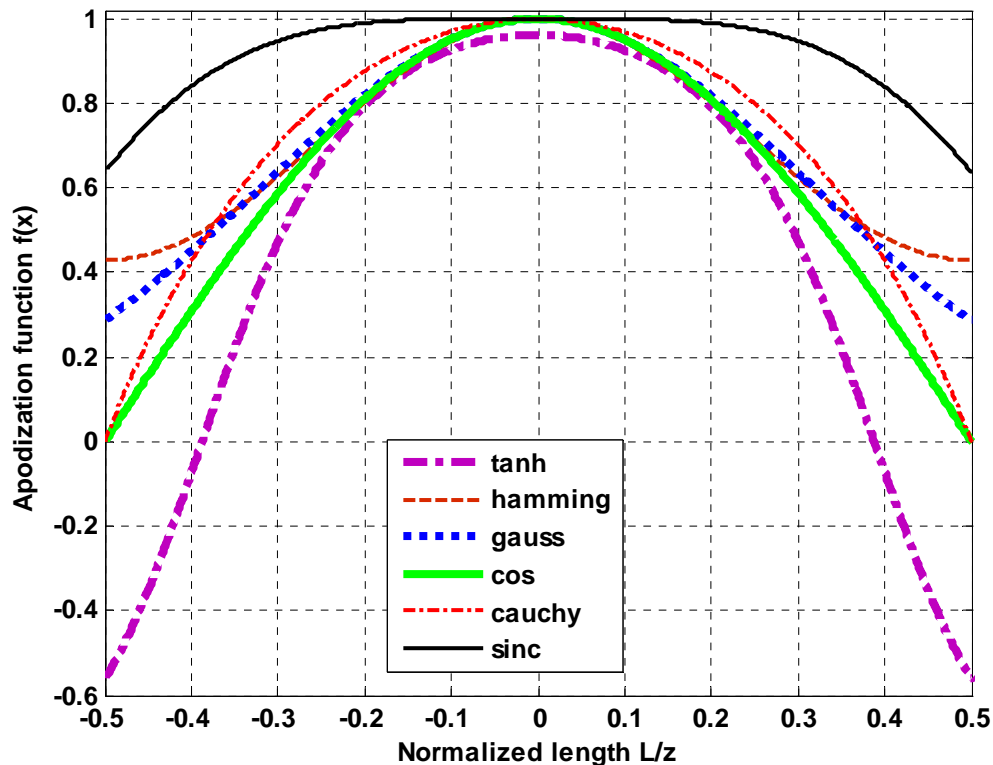


Fig. 4.9 Apodization function versus normalized length for *Tanh* ($\alpha=1$, $\beta=4$), Hamming ($H=0.8$), Gauss ($G=0.5$), *Cosine* ($A=0.15$), *Cauchy* ($B=0.2$), *sinc* ($X=1$, $Y=3$).

4.3 Determination of FBG Grating Length

For different grating lengths different amplitude of reflectivity can be obtained. As shown in Table 4.2 the reflectivity increases with the elevation of gratings length. The reflectivity for different gating length for *sinc* apodization profile has been investigated to

get best fit grating length L_g for dispersion compensation. The fiber grating achieved 56.21% reflectivity for smaller grating length of 4 cm as shown in Fig. 4.10. For $L_g = 7$ cm reflectivity is 87.53% as shown in Fig.4.11. The reflectivity increases with the increase of gratings length demonstrated in figures. For the grating length $L_g = 10$ cm the reflectivity is 96.95% as shown in Fig. 4.12. From the Fig. 4.13 it is found that for the grating length 12 cm reflectivity is about 98.83%. The fiber grating achieved more than 99% reflection when the grating length is 10 cm and maintained this value for the longer grating length.

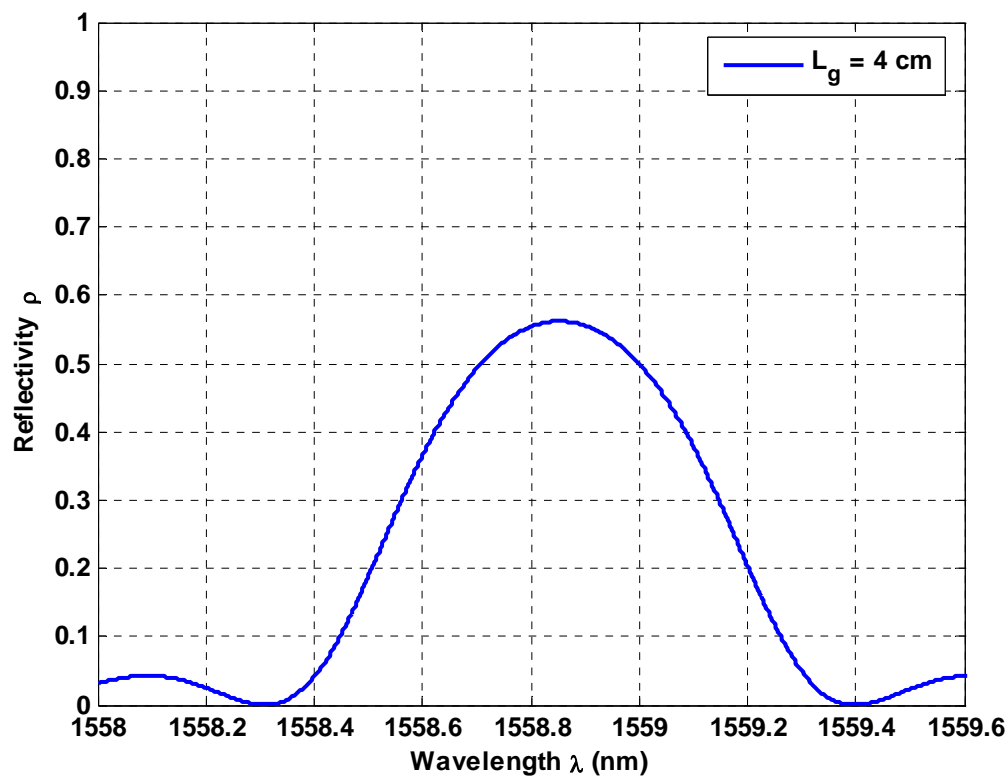
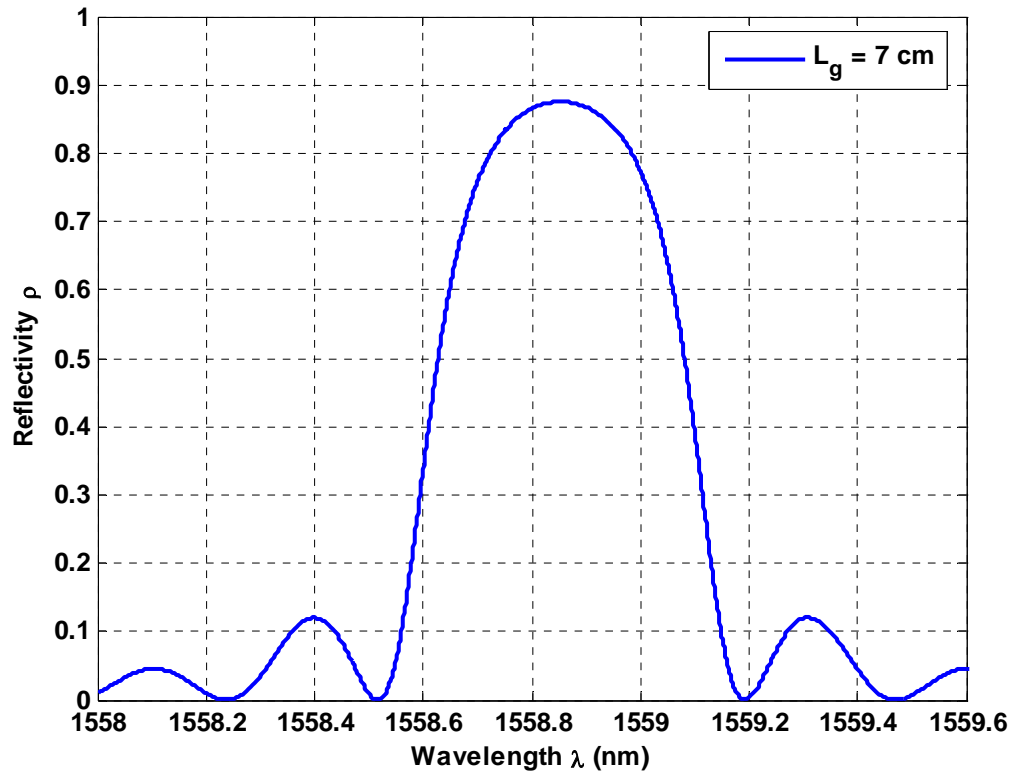


Fig. 4.10 Reflectivity versus wavelength for 4 cm of grating length for *sinc* profile.



. Fig.4.11 Reflectivity versus wavelength for 7 cm of grating length for *sinc* profile

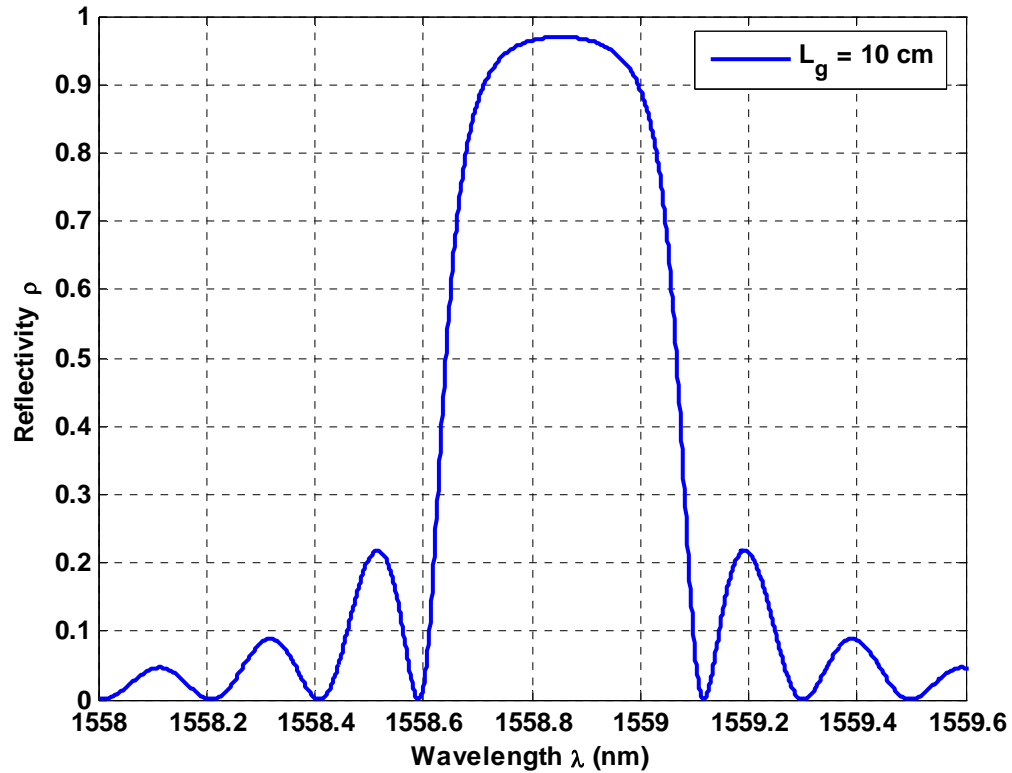


Fig.4.12 Reflectivity versus wavelength for 10 cm of grating length for *sinc* profile.

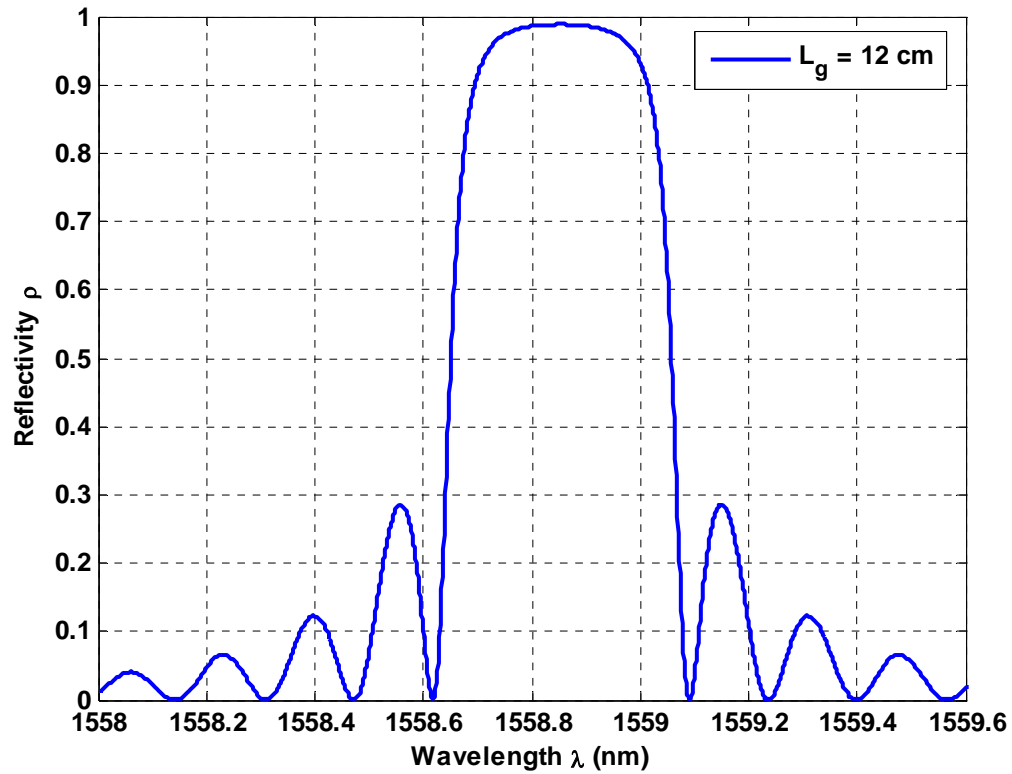


Fig.4.13 Reflectivity versus wavelength for 12 cm of grating length for *sinc* profile.

Table 4.2 Relationship between fibers Bragg grating's grating length and reflectivity.

Grating Length (cm)	Reflectivity ρ					
	<i>tanh</i>	hamming	Gauss	<i>cos</i>	Cauchy	<i>sinc</i>
1.0	7.48	6.54	0.05	23.48	2.92	5.68
1.5	15.83	13.95	0.01	43.61	6.41	12.198
2.0	25.916	23.06	0.14	61.61	11.03	20.35
2.5	36.68	33.00	0.22	75.24	16.53	29.428
3.0	47.19	42.98	0.28	84.58	22.66	38.76
3.5	56.88	52.41	0.35	90.06	29.16	47.81
4.0	65.38	60.92	0.40	94.35	35.79	56.21
5.0	72.58	68.34	1.53	96.63	42.36	63.72
6.0	78.52	74.63	4.51	98.00	48.70	70.27
7.0	87.13	84.09	21.65	99.30	60.25	87.53

Grating Length (cm)	Reflectivity ρ					
	<i>tanh</i>	hamming	Gauss	<i>cos</i>	Cauchy	<i>sinc</i>
8.0	92.44	90.02	54.51	99.75	69.92	92.14
9.0	95.61	94.64	83.39	99.91	77.64	95.09
10.0	96.44	96.64	96.03	99.97	83.61	96.95
12.0	98.55	97.88	99.32	99.98	88.10	98.83
15.0	99.53	99.25	99.99	99.998	93.84	99.72
20.0	99.91	99.84	99.99	99.999	97.77	99.97

Fig. 4.14 shows the relationship between reflectivity and grating length for *sinc* profile. From Fig. 4.14 it found that the reflectivity raised more than 96.5% for $L_g = 10$ cm and for $L_g = 12$ cm it is about 99%. Fig. 4.15 shows the relationship between reflectivity and grating length for six different apodization profiles, *Tanh* ($\alpha=1, \beta=4$), *Hamming* ($H=0.8$), *Gauss* ($G=0.5$), *Cosine* ($A=0.15$), *Cauchy* ($B=0.2$), *sinc* ($X=1, Y=3$). From Table 4.2 and Fig. 4.15 it may be inferred that grating length of 10 cm can be used for compensating dispersion of fiber Bragg grating because at this length the reflectivity is more than 96% for all apodization functions except *Cauchy*. Beyond this grating length though reflectivity is higher but it is needed to lengthen the grating length. But there is a question of phase mask to fabricate the FBG. Longer the grating length higher the cost will be to fabricate it.

Fig. 4.16 shows dispersion coefficient versus wavelength using linearly chirped *sinc* apodized FBG for different grating length. It is observed that for wavelength of 1558.8 nm and gating length $L_g = 7$ cm dispersion get $D_p = -50$ ps/nm and for $L_g = 10$ cm $D_p = -80$ ps/nm. It is also found that the value of dispersion increases to $D_p = -110$ ps/nm for grating length increases to $L_g = 11$ cm. For $L_g = 12$ cm dispersion is $D_p = -140$ ps/nm. The Fig. 4.16 it is also shows that dispersion is decreasing for higher wavelength. So, it is better to use grating length of 10 cm for dispersion compensation.

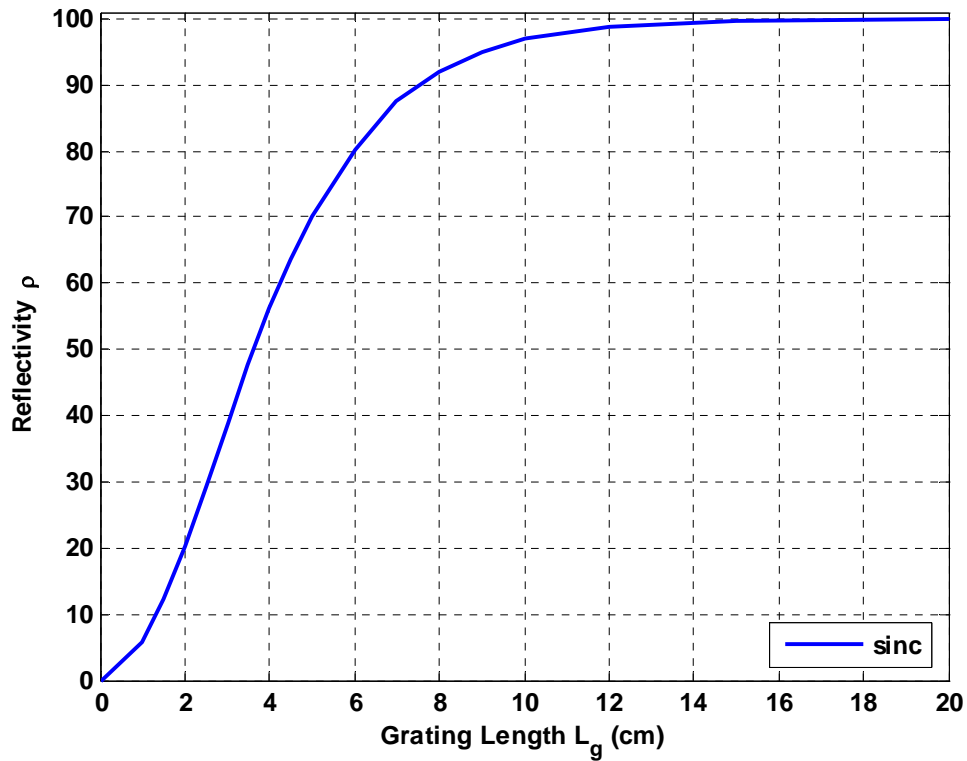


Fig. 4.14 The relationship between reflectivity and grating length for *sinc* profile.

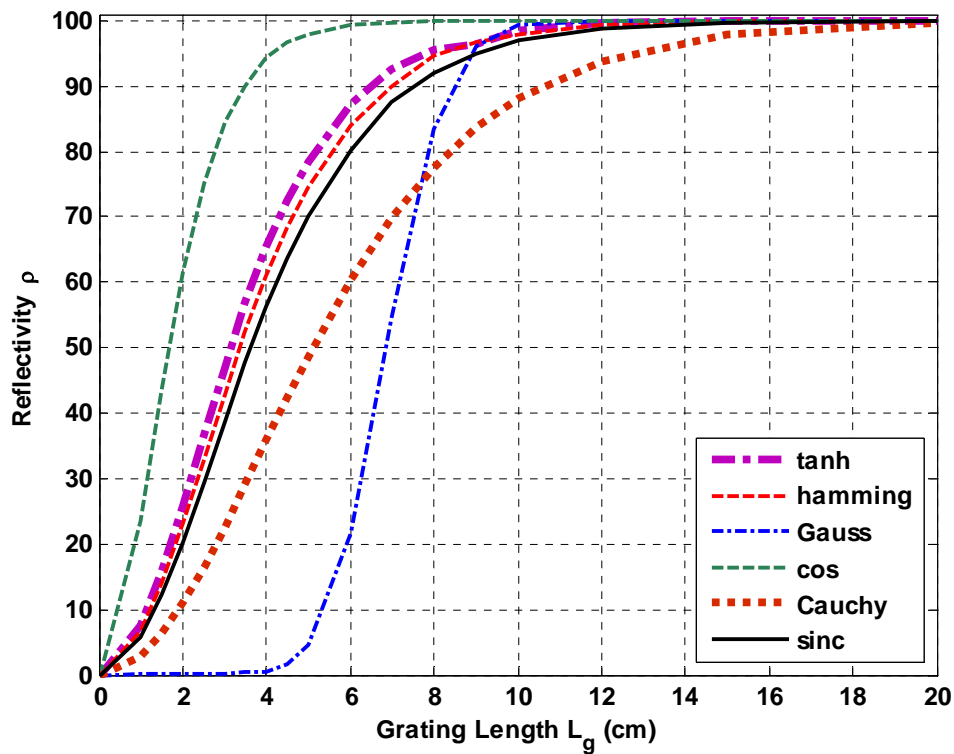


Fig. 4.15 The relationship between reflectivity and grating length for *tanh* ($\alpha=1$, $\beta=4$), *hamming* ($H=0.8$), *Gauss* ($G=0.5$), *cosine* ($A=0.15$), *Cauchy* ($B=0.2$), *sinc* ($X=1$, $Y=3$) apodization profiles.

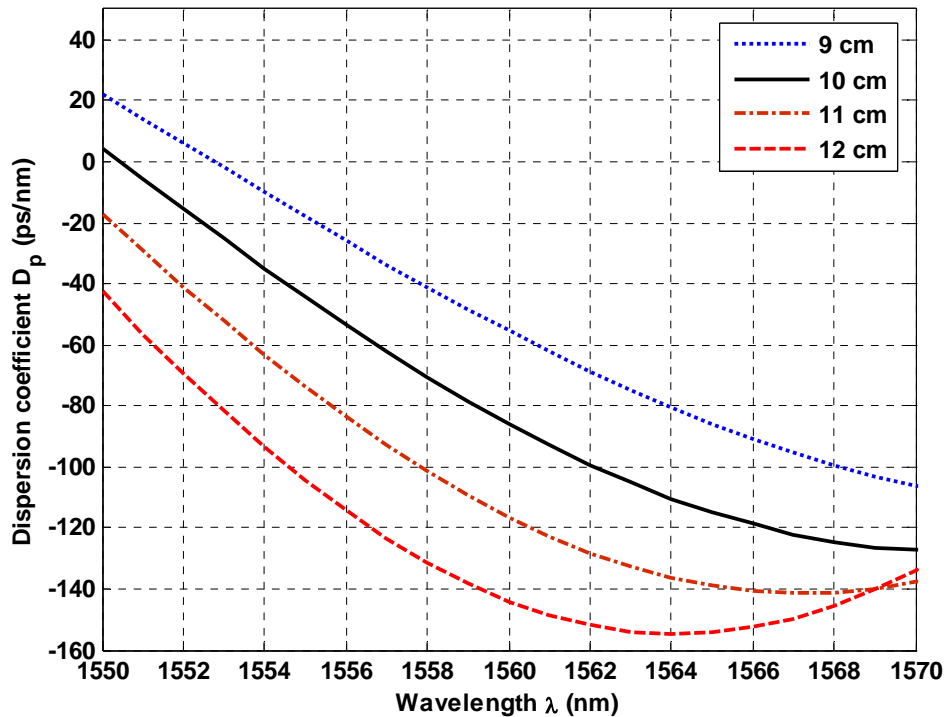


Fig. 4.16 Dispersion coefficient versus wavelength using linearly chirped *sinc* apodized FBG for different grating length.

4.4 Dispersion Compensation

To design a linearly chirped apodized FBG the grating period Λ is varied linearly. The grating length L_g divided into many small segments. By setting initial grating period $\Lambda_1=1.6$ mm, the number of segment $N = 200$ and decreasing parameter $M = 0.99$ mm, and by using geometric series the total grating length L_g is calculated. As the Bragg wavelength is represented by $\lambda_B = 2n_{eff}\Lambda_B$, Here we varied grating period Λ_B linearly then the Bragg wavelength λ_B also varied, as shown in Fig. 4.17, where different wavelength is reflected from different length of grating period.

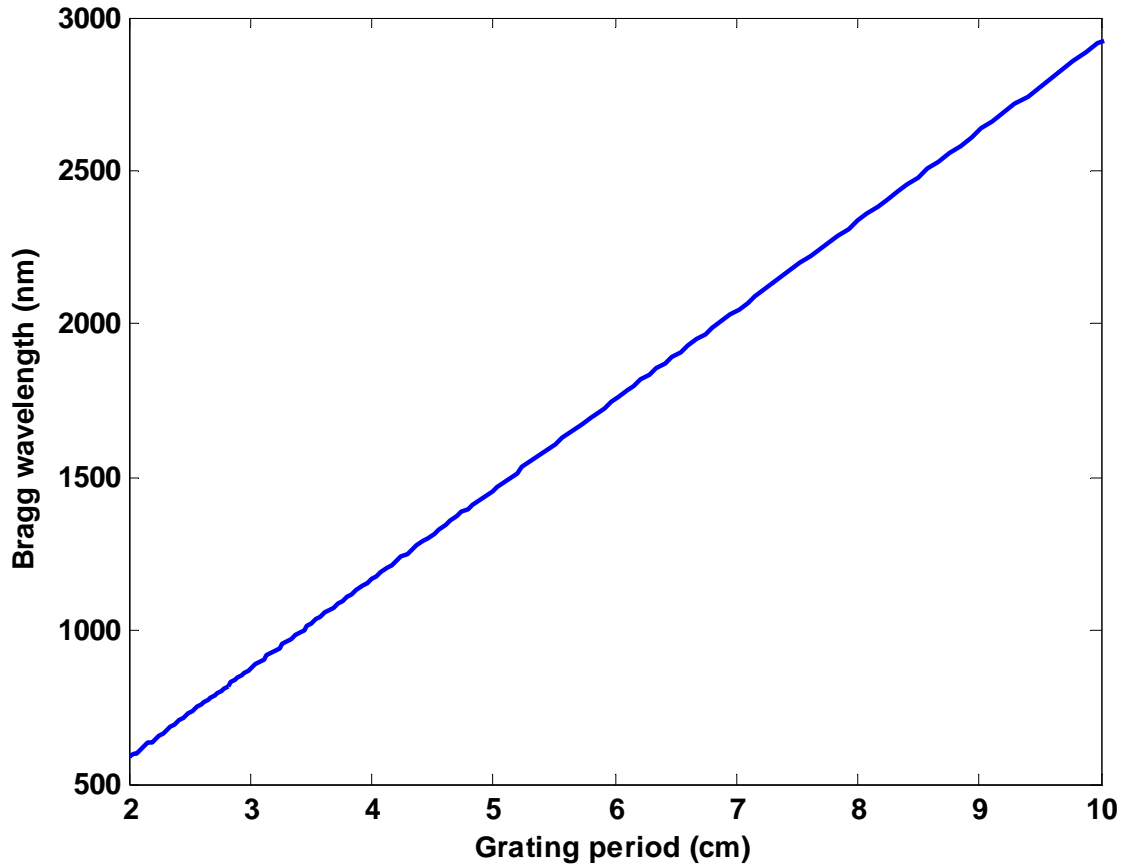


Fig. 4.17 Linearly chirped grating period (with 200 segment, length of 1st period is 1.6 mm, and linearly decrease by a factor of 0.99 mm) versus Bragg wavelength.

An analytical model has been developed to compensate first order group velocity dispersion or 2nd order dispersion β_2 and second order group velocity dispersion or 3rd order dispersion β_3 . By using effective index 1.46 and grating length $L_g = 10$ cm, 2nd order dispersion versus wavelength is plotted in Fig. 4.18. It is found that the plot is linearly increasing. For 1558 nm of wavelength $\beta_2 = 8$ ps²/km. 3rd order dispersion β_3 versus wavelength is plotted in Fig. 4.19. From the figure it is found that the β_3 is decreasing linearly as the wavelength is increasing. For the wavelength of 1558 nm the value of β_3 is -0.11 ps³/km.

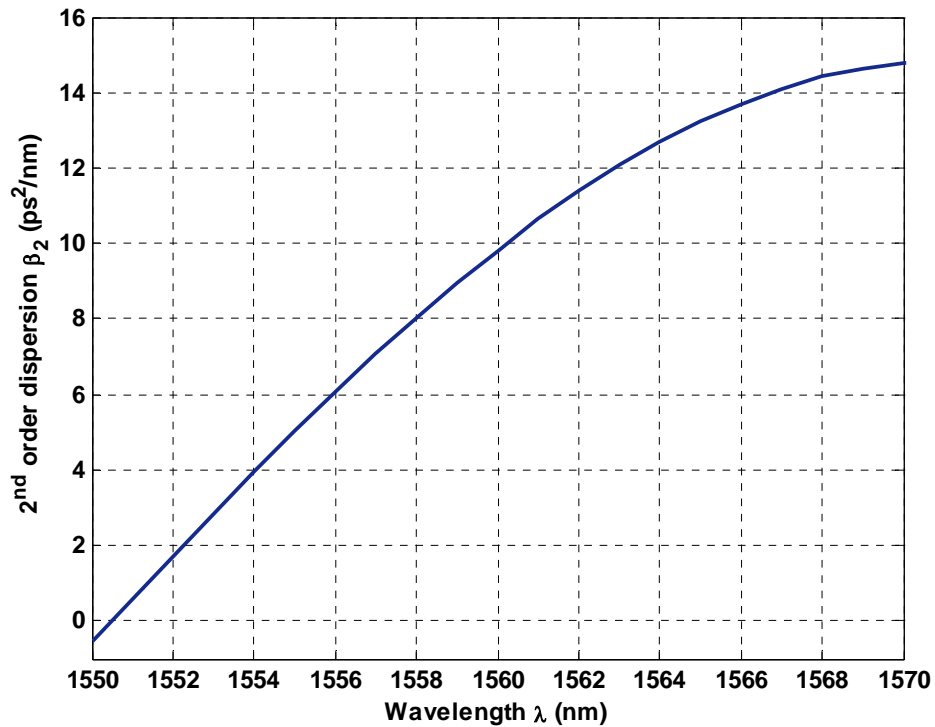


Fig 4.18 2nd order dispersion (β_2) versus wavelength using linearly chirped *sinc* apodized FBG

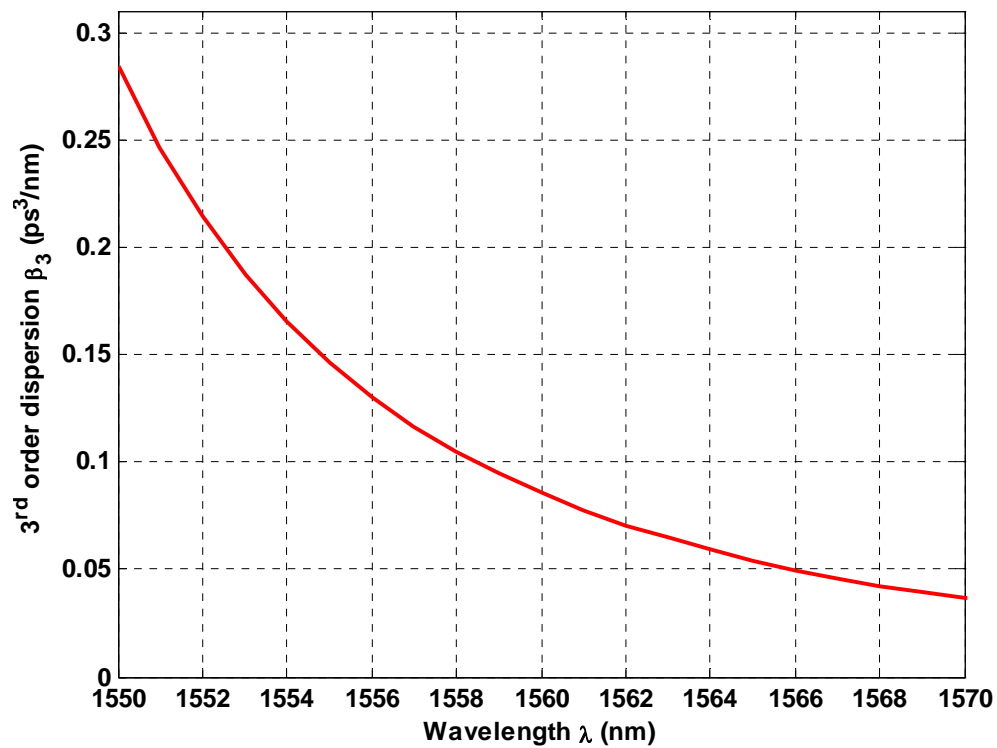


Fig.4.19 3rd order dispersion (β_3) versus wavelength using linearly chirped *sinc* apodized FBG

Figure 4.20 shows the pulse broadening factor caused by the effect of chromatic dispersion in standard single mode fiber (SSMF) transmission system, operating at the data rates of 10 Gbps and 40 Gbps while the input power is 60 mW. At bit rate 10 Gbps the pulse broadening factor is almost constant up to distance 50 km, while at 40 Gbps it is only 3 km. At 10 Gbps pulse broadening factor becomes double at 180 km, while it is 10 km at 40 Gbps. The width of the pulse get 8 times of the initial width at 700 km when system operate at 10 Gbps but it is only 45 km when the system operating at 40 Gbps.

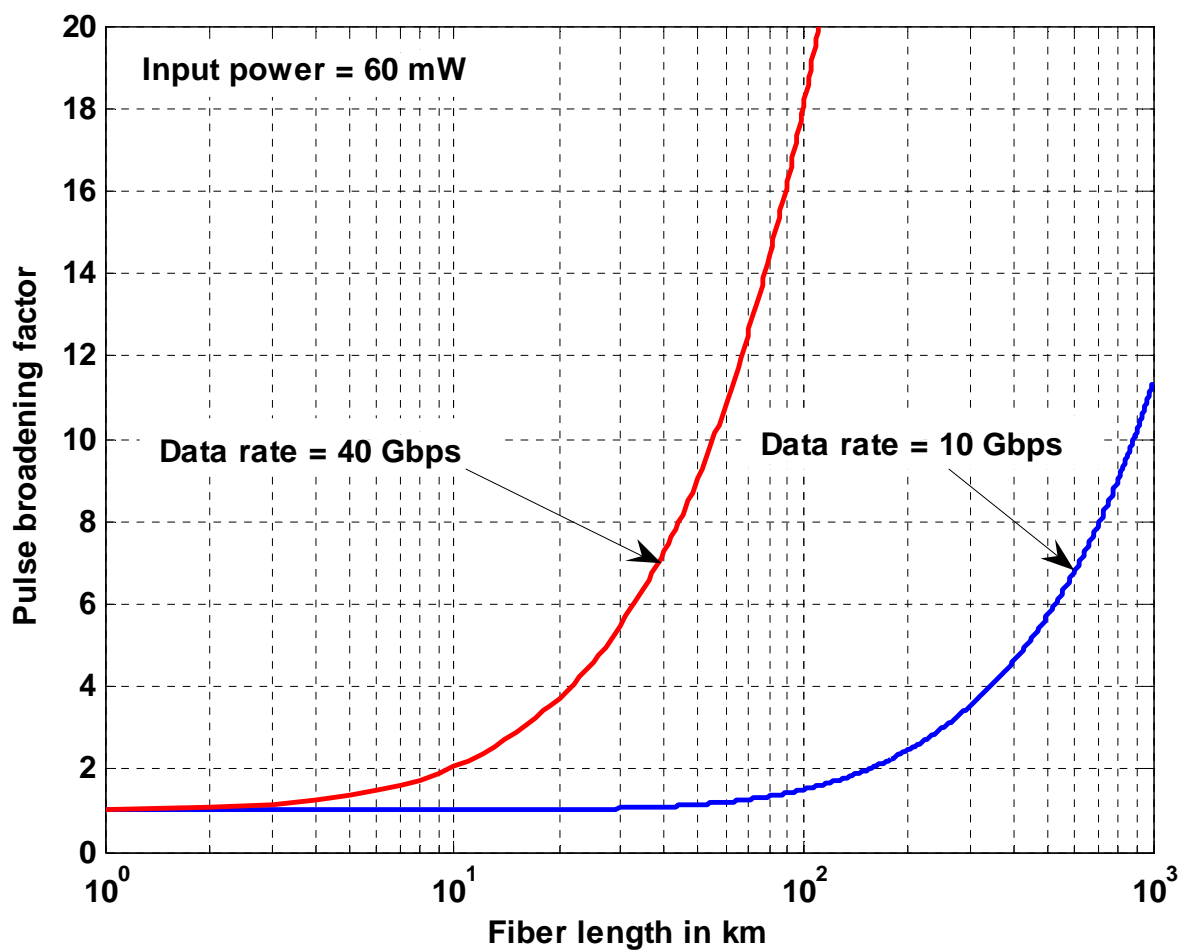


Fig. 4.20 Pulse broadening factor in SSMF fiber as a function of link length operating at bit rates 10 Gbps and 40 Gbps with 60 mW input power considering the effect of β_2 .

Figure 4.21 shows the pulse broadening factor caused by the effect of both first order β_2 and second order β_3 chromatic dispersion in SSMF transmission system, operating at the data rates of 10 Gbps while the input power is 60 mW. At bit rate 10 Gbps the pulse broadening factor is almost constant up to distance 50 km. Pulse broadening factor shows the same results for smaller link length up to 150 km but the effect of β_3 become significant after this point. The width of the pulse is more than 5 of the initial width at 300 km when considering the effect of both β_2 and β_3 , while for considering only β_2 it is 3.5.

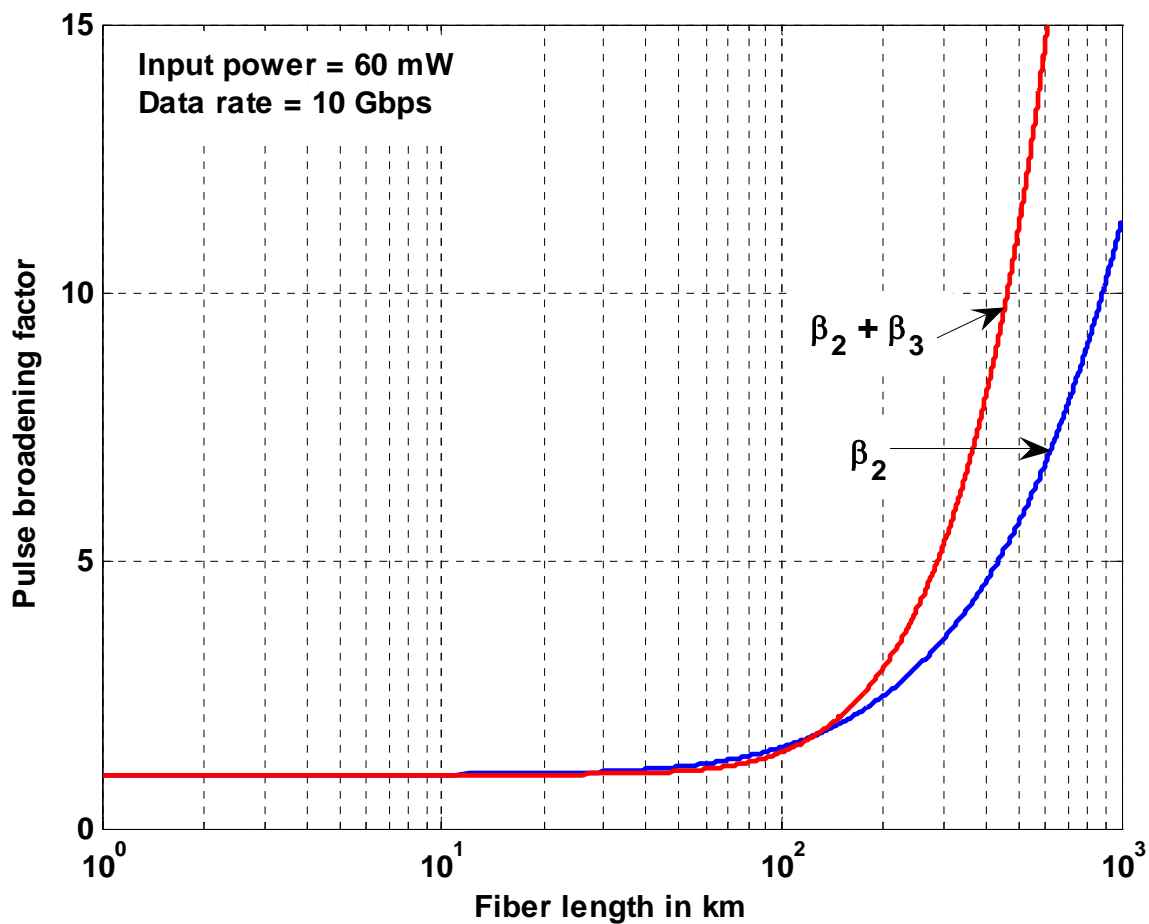


Fig. 4.21 Pulse broadening factor in SSMF fiber as a function of link length operating at bit rates 10 Gbps with 60 mW input power considering both β_2 and β_3 .

Figure 4.22 shows the pulse broadening factor caused by the effect of both first order and second order chromatic dispersion in standard single mode fiber (SSMF) optical

transmission system, operating at the data rates of 40 Gbps while the input power is 60 mW. At bit rate 40 Gbps the pulse broadening factor is almost constant up to distance 9 km. Pulse broadening factor shows the same results for smaller link length up to 5 km but the effect of β_3 become significant after the point. At link length 200 km the pulse broadening factor is 35 when considering only β_2 . But it is 44 when considering both β_2 and β_3 .

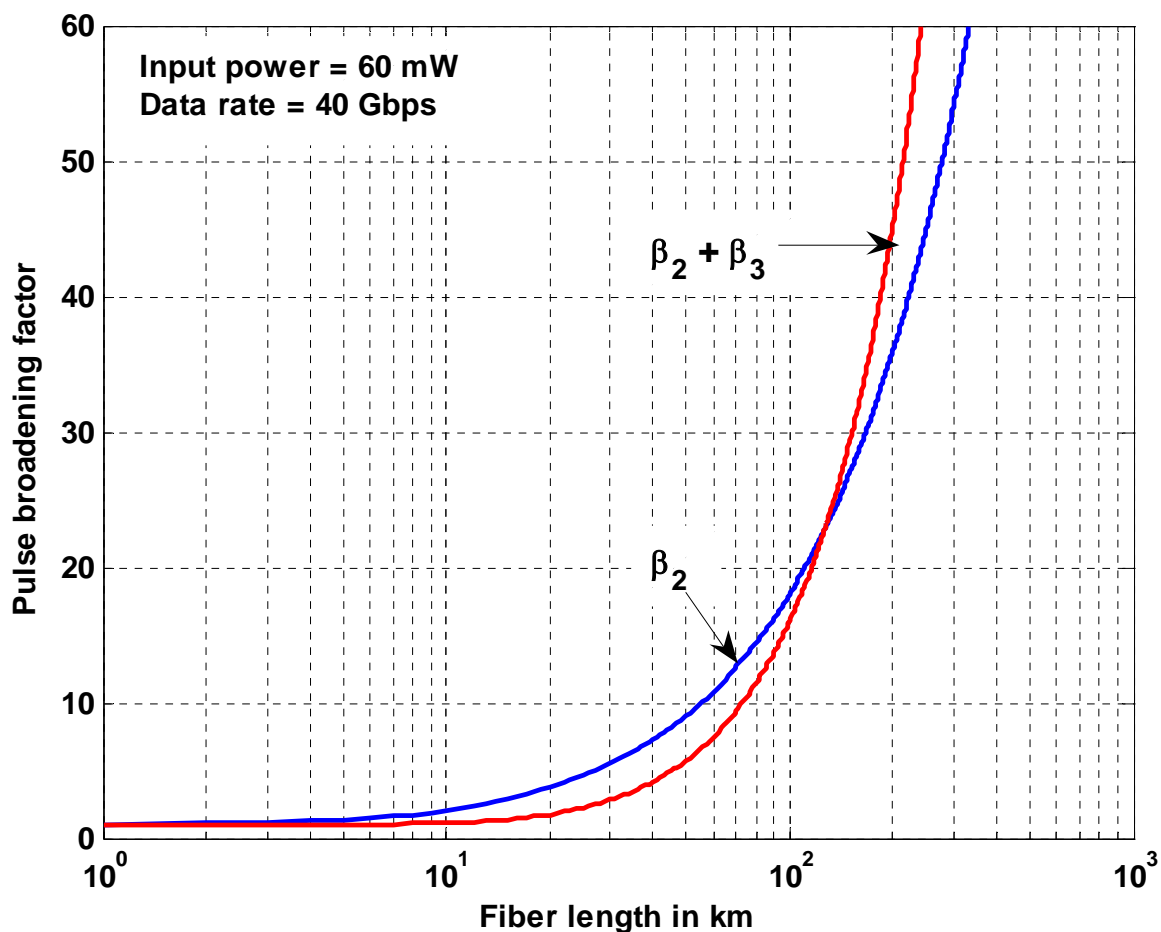


Fig. 4.22 Pulse broadening factor in SSMF fiber as a function of link length operating at bit rates 40 Gbps with 60 mW input power considering both β_2 and β_3 .

Figure 4.23 shows the pulse broadening factor of a dispersive fiber operating at 10 Gbps bit rate. From the figure it can be found that after traveling 200 km, pulse broadened at a factor of 2.5. When a linearly chirped *sinc* apodized FBG is introduced in the

communication link, then after traveling 200 km, pulse broadened at a factor of 1.5. So, pulse broadening factor is decreased.

Figure 4.24 shows the pulse broadening factor of a dispersive fiber operating at 40 Gbps bit rate. From the figure it can be found that after traveling 200 km, pulse broadened at a factor of 36. When a linearly chirped *sinc* apodized FBG is introduced in the communication link, then after traveling 200 km, pulse broadened at a factor of 20. An improvement in pulse broadening factor is found for both 10 Gbps and 40 Gbps of data rate.

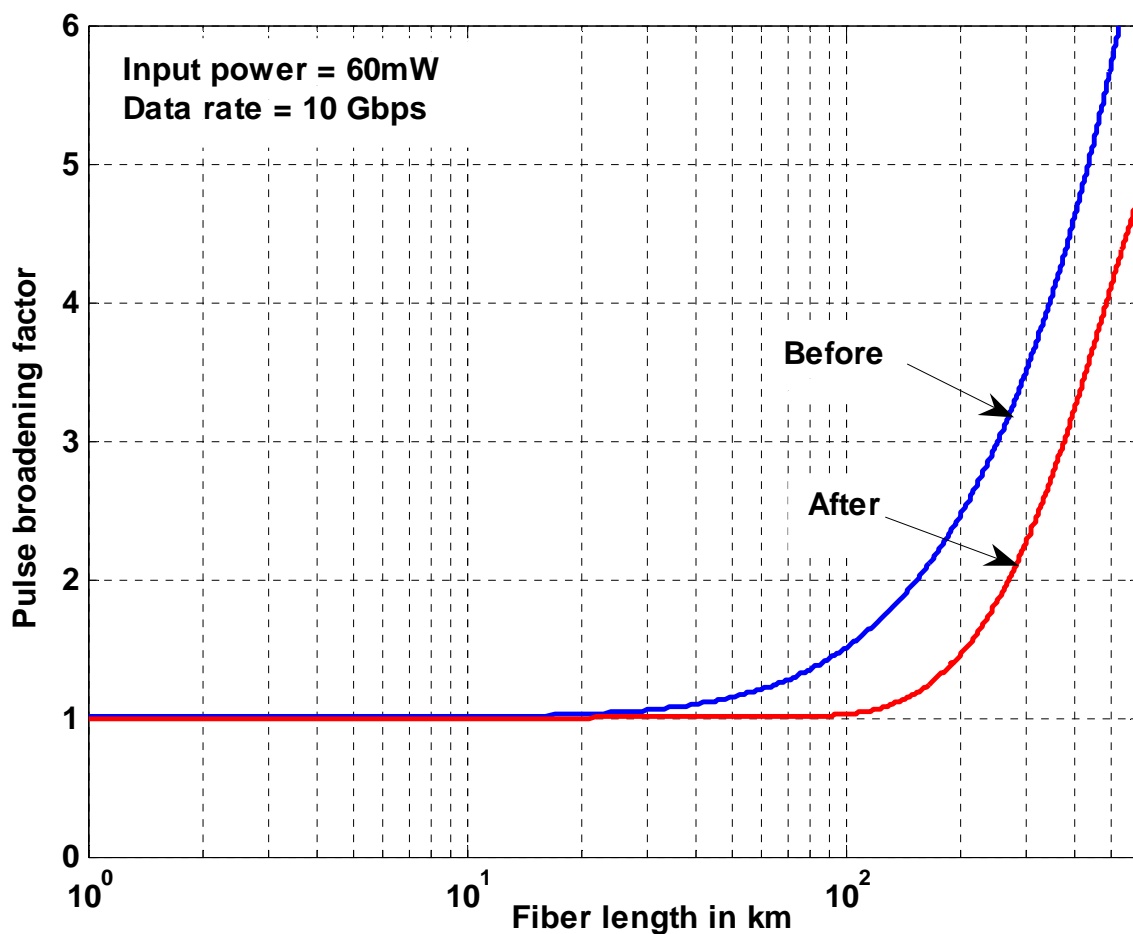


Fig. 4.23 Pulse broadening factor in SSMF fiber is as a function of link length operating at bit rates 10 Gbps with 60 mW input power before and after cascading FBG in fiber link length.

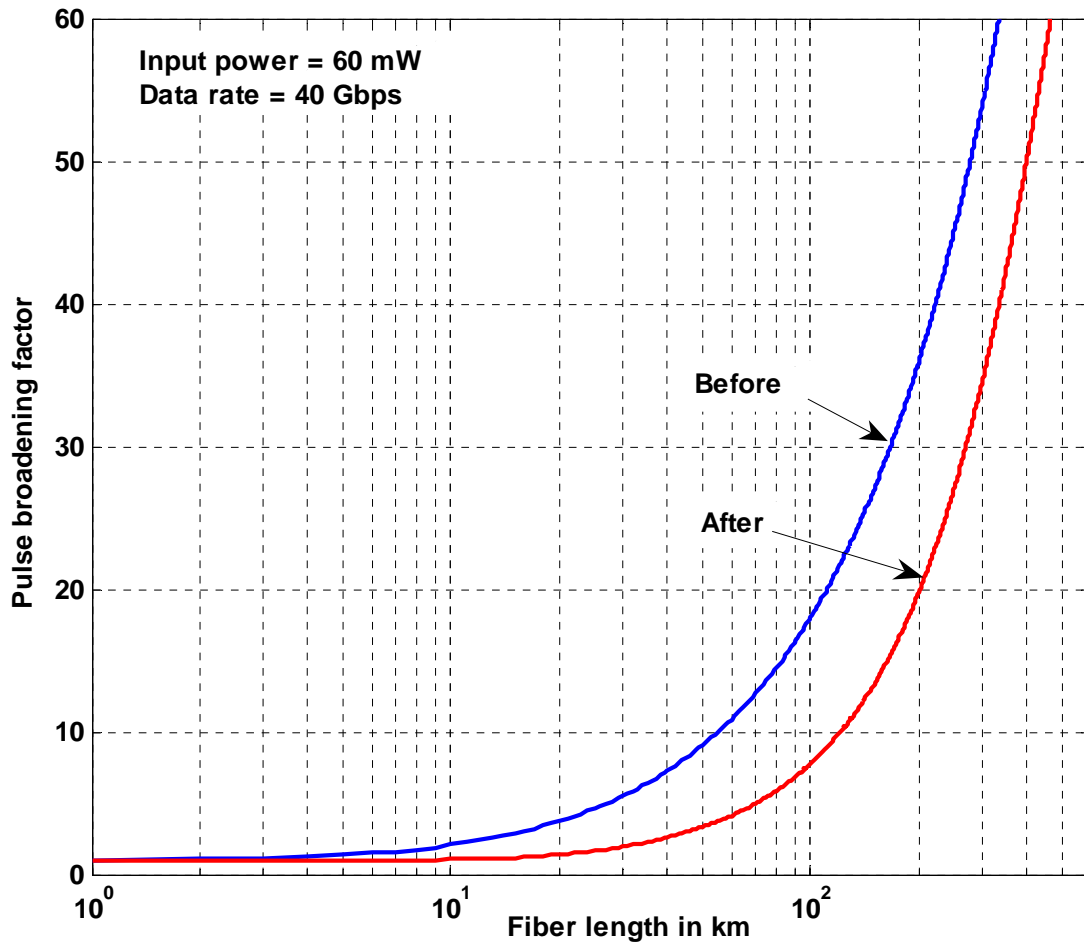


Fig. 4.24 Pulse broadening factor in SSMF fiber is as a function of link length operating at bit rates 40 Gbps with 60 mW input power before and after cascading FBG in fiber link length.

In previous chapter an analytical model for compensating dispersion coefficient D_p has been developed. MATLAB is used to simulate the analytical model. Dispersion coefficient versus wavelength for linearly chirped *sinc* apodized FBG and Bragg wavelength $\lambda_B = 1550$ nm is plotted in Fig. 4.25. shows the plot of dispersion coefficient versus wavelength for linearly chirped apodized FBG grating period with 200 segment, length of 1st period is 1.6 mm, and linearly decrease by a factor of 0.99 mm. It is found that D_p decreasing linearly as the wavelength increasing. For wavelength 1558 nm it can compensate dispersion up to -70 ps/nm.

Dispersion slope is the rate of change of Dispersion $S = \frac{dD_p}{d\lambda}$ (express in ps/nm²), is calculated analytically by using equations developed in previous chapter. From Fig. 4.26 It is found that S changes linearly for all reflected wavelength. For wavelength 1558 nm slope is about -9 ps/nm². It is found that dispersion slope is linearly increasing for every wavelength, so as the dispersion slope is increasing. Thus, such a grating with a chirp in the grating length can compensate the dispersion and dispersion slope.

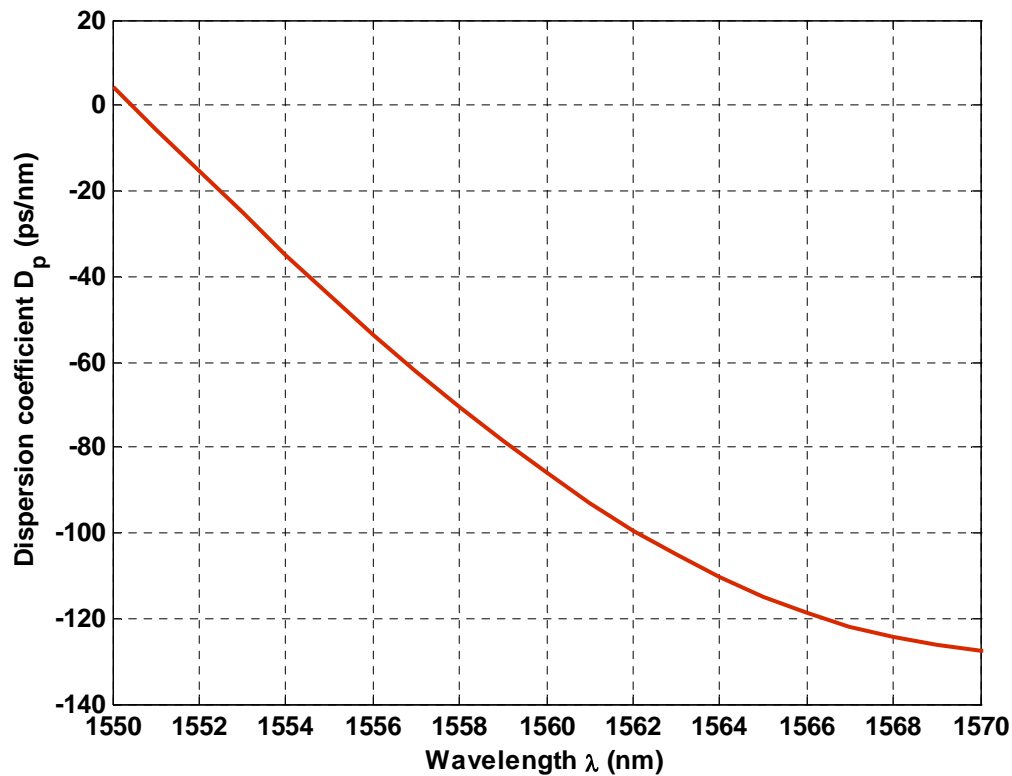


Fig. 4.25 Analytically calculated dispersion coefficient versus wavelength using linearly chirped *sinc* apodized FBG

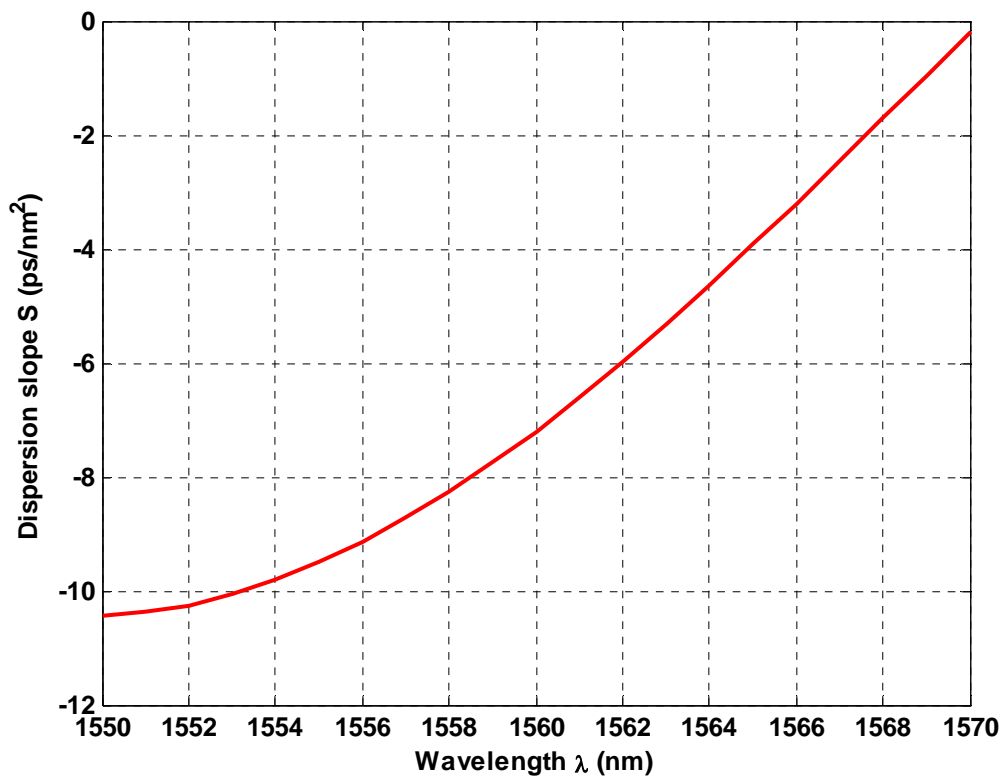


Fig. 4.26 Analytically calculated dispersion slope versus wavelength using linearly chirped *sinc* apodized FBG

Fig. 4.27 shows the relationship between unapodized FBG and sinc apodized FBG for dispersion compensation. From the Fig. 4.27 it is found that at the wavelength 1558.8 nm the dispersion coefficient $D_p = -80$ ps/nm and for unapodized FBG it is $D_p = -70$ ps/nm for apodized FBG

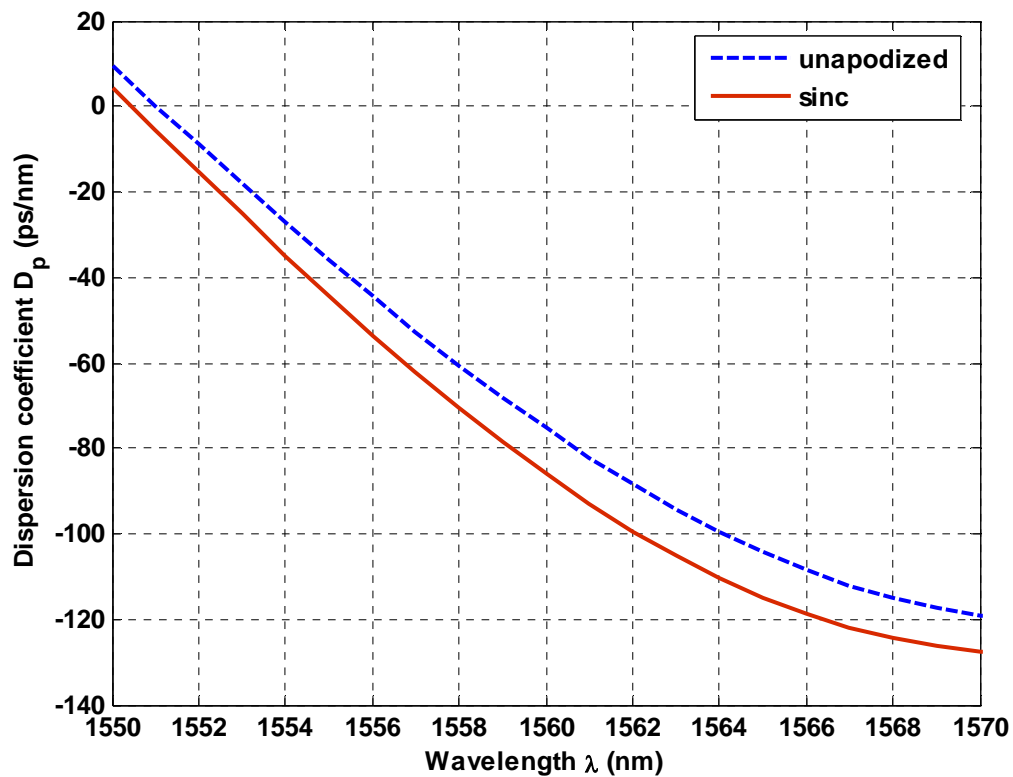


Fig: 4.27 Dispersion coefficients versus wavelength for unapodized FBG and sinc apodized FBG.

In Fig. 4.28 graphs shows the plot of reflectivity versus wavelength of a WDM system. Where the bandwidth is $\Delta\lambda = 0.2$ nm and channel spacing is 0.6 nm.

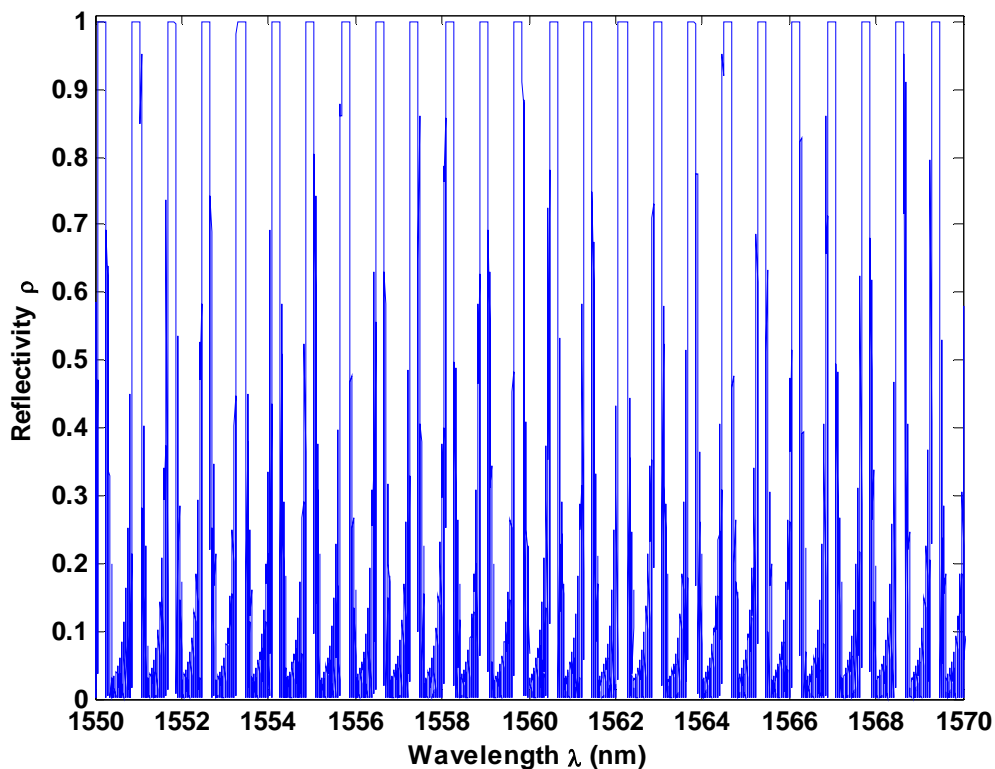


Fig: 4.28 Reflectivity spectra of a WDM system by using proposed dispersion compensation grating.

The Fig. 4.29 shows the plot of pulse regeneration obtained from linearly chirped FBG for data rate 10 Gbps. Initial, broadened and recompressed pulse after transmission through 100 km of fiber and 10 cm of fiber Bragg grating is shown. If the initial pulse propagates over fiber length $L_f = 100$ km it broadened due to dispersive properties of the optical fiber. Then the broadened pulse is fed through the proposed linearly chirped apodized FBG, the broadened pulse then recompressed about the same as input pulse as shown in Fig 4.29. The Fig. 4.30 shows the plot of pulse regeneration obtained from linearly chirped FBG for data rate 40 Gbps. Initial, broadened and recompressed pulse after transmission through 100 km of fiber and 10 cm of fiber Bragg grating is shown.

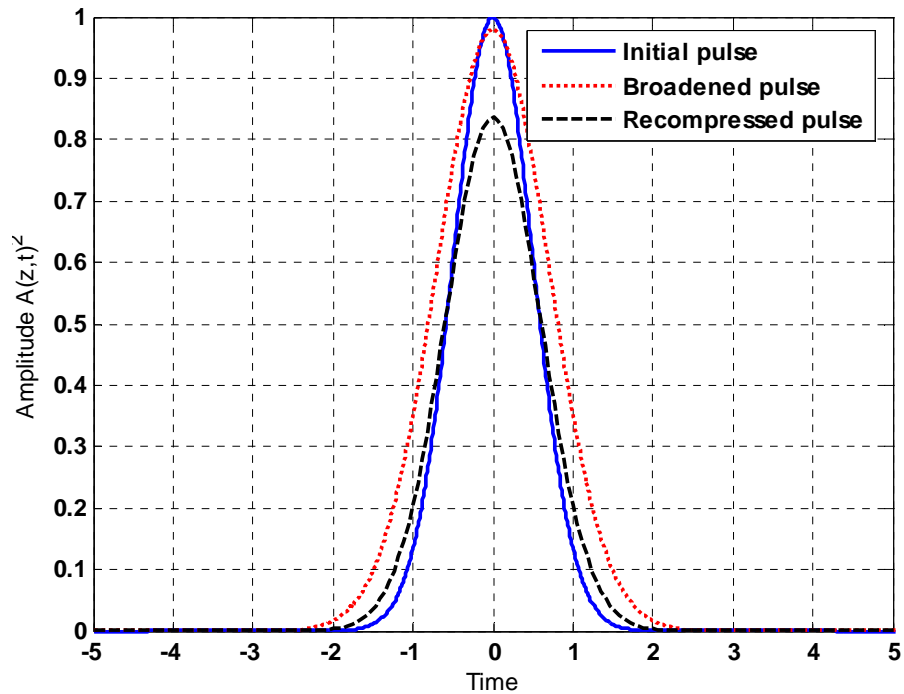


Fig. 4.29 Initial, broadened and recompressed pulse after transmission through 100 km of fiber and 10 cm of fiber Bragg grating. Data rate 10 Gbps.

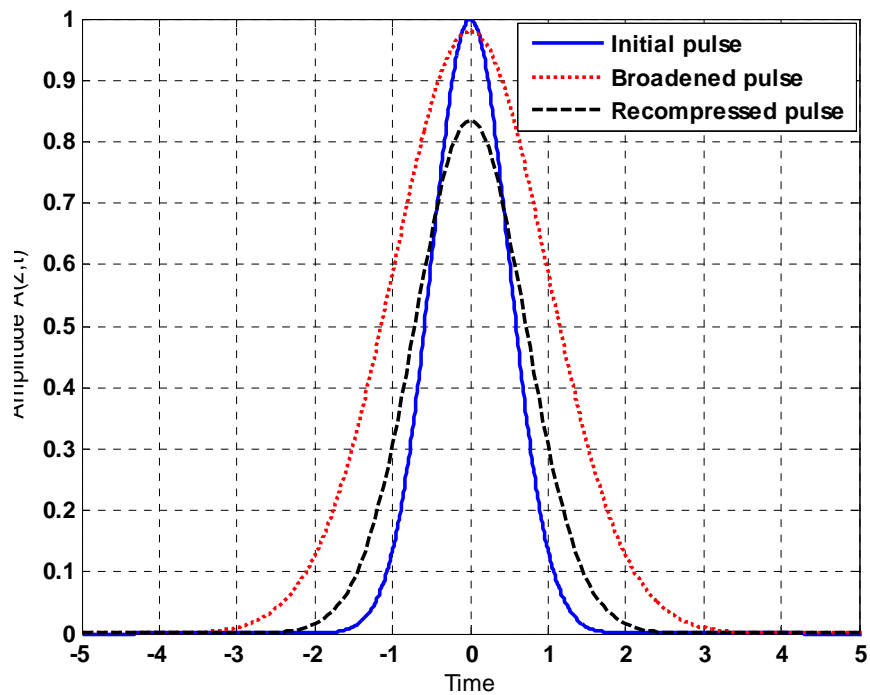


Fig. 4.30 Initial, broadened and recompressed pulse after transmission through 100 km of fiber and 10 cm of fiber Bragg grating. Data rate 40 Gbps.

4.5 Comparison with Contemporary Works

Dispersion is numerically calculated by using Centered Finite Divided Difference formula. The analytical model for dispersion is simulated by using MATLAB. A comparison between the numerically calculated values and the MATLAB simulation results of the analytical model has been shown in Fig. 4.31. Both the results are almost same. This validates the proposed analytical model.

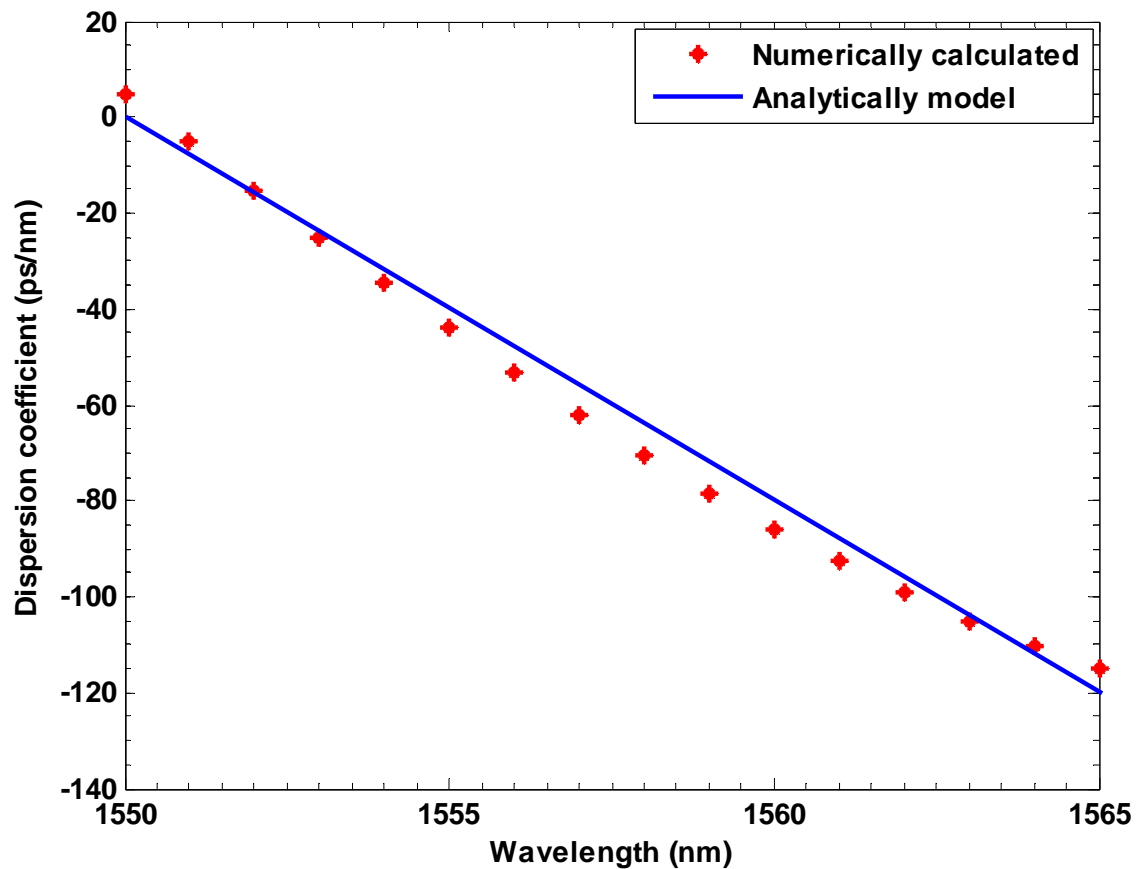


Fig. 4.31 Comparison between numerically calculated values with analytical model for dispersion coefficients versus wavelength.

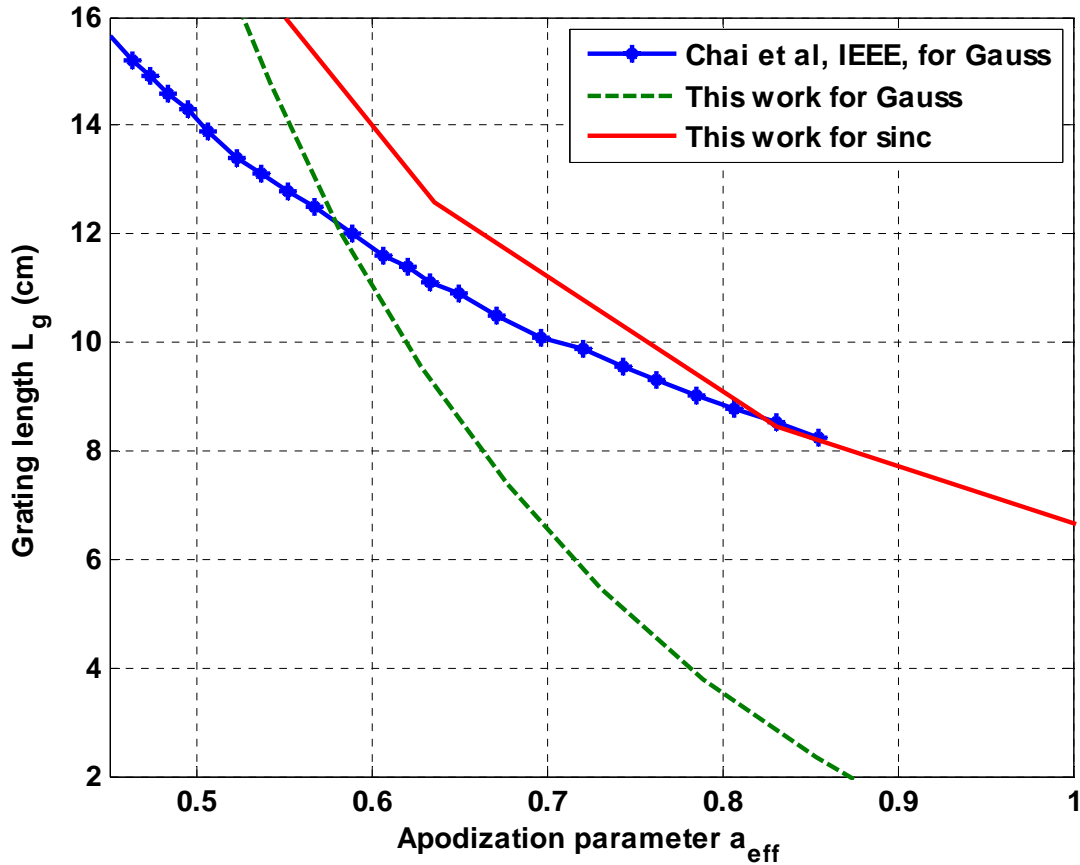


Fig. 4.32 Comparison of simulation results of this work with the already published data in Ref. [5].

Simulation results of Gauss and *sinc* functions with the existing published data of Fig. 2 in [5] for Gauss function is compared in Fig. 4.32. Chai et al used control parameter of Gauss profile ($D = 0.27$), while in this study for Gauss ($G = 0.50$) and for *sinc* ($X = 1$, $Y = 3$) are used. It is observed that for grating length of 10 cm, from the works in [5], the apodization parameter value obtained is 0.7, but from this work, the apodization parameter values obtained are more than 0.75 and 0.62 respectively for the *sinc* and Gauss functions. As the maximum apodization parameter a_{eff} is preferred, so, it can be proposed that *sinc* function shows superior performance at a grating length of 10 cm.

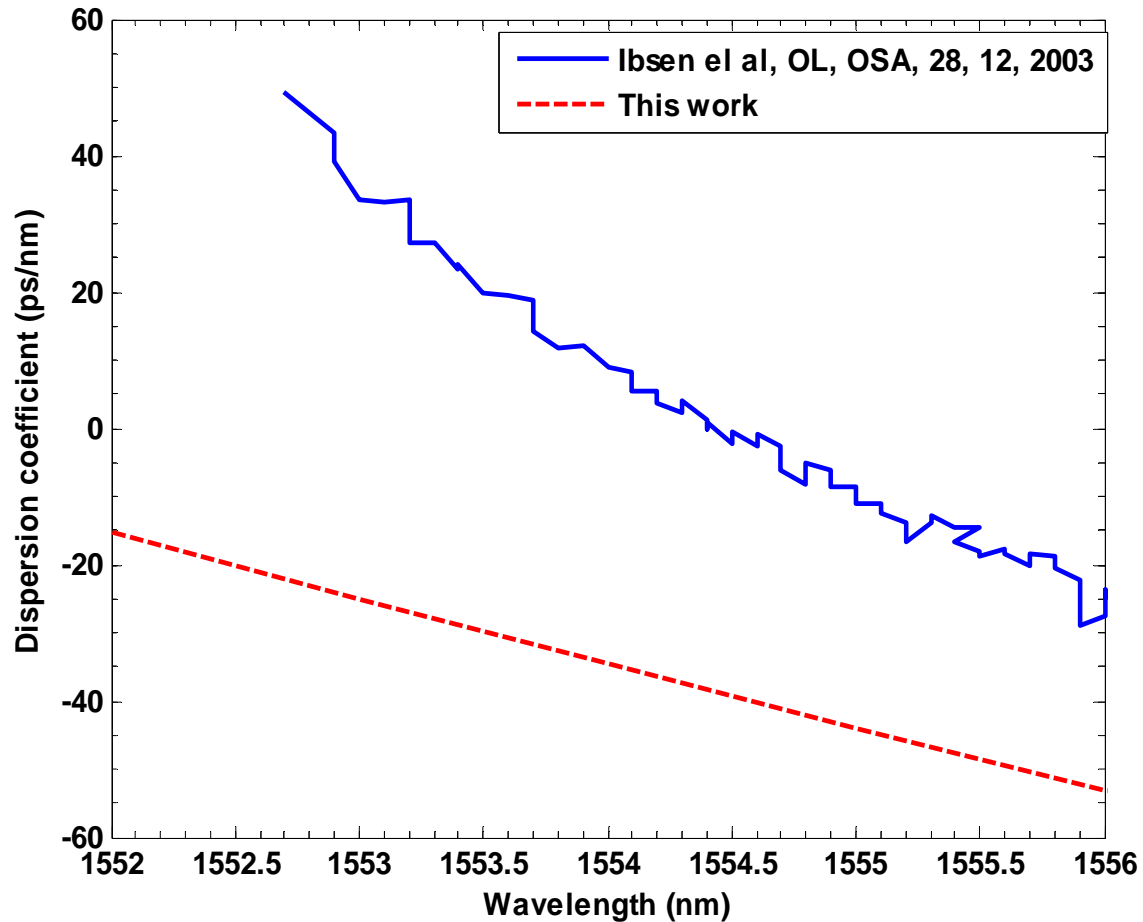


Fig. 4.33 Comparison of simulation results of this work with experimental data the published in Ref. [13].

Comparison of the MATLAB simulation results of the proposed analytical model with the experimental data already published in the literature [13] is shown in Fig. 4.33. Ibsen et al used $\kappa = 2600 \text{ m}^{-1}$ and $n_{\text{eff}} = 1.3$ while for this work $\kappa = 2290 \text{ m}^{-1}$ and $n_{\text{eff}} = 1.46$. In the literature [13] they have got reflectivity $\rho = 75\%$ but in this work reflectivity is $\rho = 97\%$ which shows the better performance. From Fig. 4.33 it is observed that the graphs follow the same decaying trend. For the wavelength of 1555.5 nm dispersion coefficient obtained from experimental work of [13] is -15 ps/nm and for this analytical model is -52 ps/nm. Dispersion slope obtained in [13] is -20 ps/nm^2 and for this work dispersion slope is -10 ps/nm^2 . So the proposed analytical model is better.

4.6 Summary

The effect of chromatic dispersion on the pulse broadening from the above graphs it can be observed that

1. For the same optical fiber link length as the data rate increases the pulse broadening factor also increases. Pulse broadened faster in shorter pulse than the longer pulse and this is due to the fact that the frequency spectrum of the shorter pulse is wider than the frequency spectrum of the wider pulse.
2. The pulse broadening factor is caused by the effect of both first order and second order chromatic dispersion. At the short link length only first order chromatic dispersion is significant, but at the higher link length second order chromatic dispersion also becomes significant.
3. To evaluate the performance of different apodization profiles of linearly chirped FBG for the dispersion compensation, six different apodization profiles: *tanh*, hamming, gauss, *cos*, Cauchy and *sinc* is considered. In this study, the effect of the apodization profiles on reflection spectra is also explored. The analysis shows that an apodization profile '*sinc*' results overall superior performance.
4. The apodization parameter ranges is also explored it is found that for *sinc* profile it is more than 0.75. Grating length is also determined; it is found that the grating length of 10 cm is the best for dispersion compensation.
5. Analytical models have been simulated by using MATLAB that can effectively compensate the 1st order and 2nd order group velocity dispersion, dispersion coefficient and dispersion slope.
6. The comparison with contemporary works is done. It is found that the analytical model shows superior performance.

Chapter 5

Conclusions

5.1 Conclusions

In this chapter, the conclusions is summarized that can be drawn from the research performed for this dissertation, then provide suggestions for future research.

A detailed theoretical analysis is carried out to get an expression of pulse broadening factor for a Gaussian pulse that is affected by the combined effects of first order and second order chromatic dispersion in an optical fiber communication system. While analyzing the effect of chromatic dispersion on pulse broadening it is found that the pulse broadening factor increases with an increase of bit rate. For example in the case of standard single mode fiber (SSMF) for 10 Gbps pulse broadening factor becomes double at 180 km, while it is 10 km at 40 Gbps.

The pulse broadening factor is caused by the effect of both first order and second order chromatic dispersion. At the short link length only first order chromatic dispersion is significant, but at the higher link length second order chromatic dispersion becomes significant. For example in the case of SSMF the width of the pulse is 5 of the initial width at 200 km when considering the effect of both β_2 and β_3 , while for considering only β_2 it is 3.5.

The performance evaluated of different apodization profiles of LCFBG for the dispersion compensation. Here six different apodization profiles: *tanh*, hamming, Gauss, *cos*, *Cauchy* and *sinc* is considered. In this study, the effect of the apodization profiles on reflection spectra is also explored. The analysis shows that an apodization profile '*sinc*' results overall superior performance. As *sinc* profile shows more than 96.95% reflectivity

with minimum sidelobe, which is a desired condition. To get largest possible values of apodization parameter a_{eff} , six different apodization profiles: *tanh*, hamming, gauss, *cos*, *Cauchy* and *sinc* is investigated. Among all profile *sinc* profile shows the biggest value of a_{eff} . Reflectivity for various grating length is also investigated to get optimal grating length. It could derive to decision that grating length 10 cm can be used for dispersion compensating FBG.

An analytical formulation have been developed that can effectively compensate the second order and third order dispersion β_2 , β_3 respectively, chromatic dispersion and dispersion slope. It is found that for 1558 nm of wavelength $\beta_2 = 8 \text{ ps}^2/\text{km}$ and the value of β_3 is $-0.11 \text{ ps}^3/\text{km}$. It is found that D_p decreasing linearly as the wavelength increasing and dispersion slope is linearly increasing for every wavelength. For wavelength 1558 nm it can compensate chromatic dispersion up to $-70 \text{ ps}/\text{nm}$ and dispersion slope is $-9 \text{ ps}/\text{nm}^2$.

Initial, broadened and recompressed pulse after transmission through 100 km of fiber and 10 cm of fiber Bragg grating also investigated and found a significant improvement. Data rate 10 Gbps. Input power 60 mW. In summary, it can be demonstrated that by using linearly chirped *sinc* apodized linearly chirped FBGs of length 10 cm of apodization strength factor at ranges from 0.7 to 0.8 can compensate both dispersion and dispersion slope.

5.2 Future Scopes

Research is a continuous process. So, it is important to think about the scopes of further extension of the current research work. In this work, dispersion compensation by using apodized linearly chirped FBG has been analyzed. This work also has several possible extensions that could be attempted as on going research work. Some specific recommendations based on the present work are given in the following paragraphs.

The characteristic of proposed apodized chirped FBG can be improved by considering the effect of strain and temperature.

The total coupling coefficient of the grating has an important effect over the equalization performances; the effect of different coupling coefficient can also be investigated.

An experimental investigation can be done as future work. It is needed to establish the discrepancy between theory and experiment for the chirped apodized FBG. This would be in the form of a theoretical study as well as an experimental investigation.

References

- [1] D. K. Mynbaev and L. L. Scheiner, *Fiber Optic Communication Technology*, Pearson Education Inc., India, 2001
- [2] R. Kashyap, *Fiber Bragg Gratings*, 2nd Ed., Academic Press, USA, 2010.
- [3] S. Bandyopadhyay, P. Biswas, A. Tasipal, S. K. Bhadra and K. Dasgupta, "Empirical relations for design of linear edge filters using apodized linearly chirped fiber Bragg grating," *IEEE Journal of Lightwave Technology*, vol. 26, no. 24, pp. 3835-3859, 2008.
- [4] O. Mahran, T. A. Hamdallah, M. H. Aly and A. E. El-Samahy, "Apodized chirped fiber Bragg gratings for wavelength shift compensation under sea level," *Journal of Applied Sciences Research*, vol. 5, no. 10, pp. 1592-1603, 2009.
- [5] J. Chai, Z. Yu and Y. Liu, "Analysis of the apodization parameter of linearly chirped Bragg gratings for dispersion compensation," *Proceedings of First International Conference on Communications and Networking*, China, pp. 1-5, 2006.
- [6] S. Doucet, S. LaRochelle and M. Morin, "Reconfigurable dispersion equalizer based on phase-apodized fiber Bragg gratings," *IEEE Journal of Lightwave Technology*, vol. 26, no. 16, pp. 2899-2908, 2008.
- [7] M. Li and H. Li, "Reflection equalization of the simultaneous dispersion and dispersion slope compensator based on a phase only sampled fiber Bragg gratings," *Optics Express*, vol. 16, no. 13, pp. 9821-9828, 2008.
- [8] S. P. Ho, A. Jalil, A. R. Rosly and A. T. Bashir, "Fiber Bragg grating modeling, simulation and characteristics with different grating lengths," *Journal of Fundamental Science*, vol. 3, pp. 167-175, 2007.
- [9] M. Hany, M. H. Aly and M. Nassr, "Dispersion compensation using tunable chirped apodized far off resonance fiber Bragg gratings in transmission," *Journal of Applied Science Research*, vol. 5, no. 10, pp. 1630-1638, 2009.
- [10] E. J. Gualda, L. C. Gomez-pavon and J. P. Torres, "Compensation of third order dispersion in a 100 Gb/s single channel system with in-line fibre Bragg gratings," *Journal of Modern Optics*, vol. 52, no. 9, pp. 1197-1206, 2005.

- [11] R. Romero, G. Rego, and P. V. S. Marques, "Apodization of fiber Bragg gratings by using arc discharges," *Microwave and Optical Technology Letters*, vol. 50, no. 2, pp. 316-119, 2007.
- [12] M. Hany, M. H. Aly and M. Nassr, "Dispersion compensation in transmission using AFBG chirped with two beam interference fringe spacing," *Journal of Applied Science Research*, vol. 5, no. 10, pp. 1622-1629, 2009.
- [13] I. Morten. and F. Ricardo, "Fiber Bragg gratings for pure dispersion slope compensation," *Optics Letters*, vol. 28, no. 12, pp. 180-182, 2003.
- [14] N. H. Sunand, J. Liau and Y. W. Kiang, "Tunable Chromatic Dispersion Compensation in 40-b/s Systems Using Nonlinearly Chirped Fiber Bragg Gratings," *Journal of Lightwave Technology*, vol. 20, no. 12, pp.2239-2246, 2002.
- [15] K.O. Hill, Y. Fujii, D.C. Johnson and B.S. Kawasaki, "Photosensitivity in optical waveguides:Application to reflection filter fabrication," *Applied Physics Literature*, vol. 32, no.10, p. 647, 1987
- [16] U. Osterberg and W. Margulis, "Efficient second harmonic in an optical fiber," in: Technical Digest of XIV Internet, Quantum Electron. Conference, paper WBB1, 1986.
- [17] R.H. Stolen, H.W.K. Tom, "Self-organized phase-matched harmonic generation in optical fibers," *Optical Lett.*, vol.12, pp. 585–587, 1987
- [18] M.C. Farries, P.J.St. Russell, M.E. Fermann, D.N. Payne, "Second harmonic generation in an optical fiber by self-written w(2) grating," *Electronics Letters*, vol. 23 (7), pp. 322–323, 1987
- [19] J. Stone, "Photorefractivity in GeO₂-doped silica fibres," *Journal of Applied Physics*, vol. 62 (11) p. 4371, 1987
- [20] J. Bures, S. Lacroix and J. Lapiere, "Bragg reflector induced by photosensitivity in an optical fibre: model of growth and frequency response," *Application of Optical*, vol.21 (19) p. 3052,1982
- [21] G. Meltz, W.W. Morey, W.H. Glenn, Formation of Bragg gratings in optical fibres by transverse holographic method, *Optical Lett.*, vol.14 (15) p. 823, 1989
- [22] J. Mora, J. Villatoro, A. Diez, J. L. Cruz and M. V. Andres, "Tunable chirp in Bragg gratings written in tapered cored fibers", *Optics Comm.*, 210, pp. 51-55, 2002.

- [23] J. Kwan, S. Chung, Y. Jeong and B. Lee, 'Group Delay tailored Chirped fiber Bragg Gratings Using a Tapered Elastic Plate', *IEEE Photon. Tech. Lett.*, 14, pp.1433-1435, 2002.
- [24] Y. Painchaud, A. Chandonnet and J. Lauzon, 'Chirped fibre gratings produced by tilting the fibre', *Electronic. Lett.*, vol. 31, pp. 171-172, 1995.
- [25] A. E. Willner, K. M. Feng, J. Cai, S. Lee, J. Peng and H. Sun, 'Tunable Compensation of Channel Degrading effects Using Nonlinearly Chirped Passive fiber Bragg Gratings', *IEEE Journ. of Selected Topics in Quantum. Electronic*, vol. 5, pp.1298-1311, 1999.
- [26] R. Kashyap, P. F. McKee, R. J. Campbell and D. L. Williams, 'Novel method of producing all fibre photoinduced chirped gratings', *Electronic. Lett.*, vol.30, pp. 996-998, 1994.
- [27] K. C. Byron and H. N. Rourke, 'Fabrication of chirped fibre gratings by novel stretch and write technique', *Electronic Lett.*, vol. 31, pp. 60-61, 1995.
- [28] Turan Erdogan, "Fiber grating spectra," *Journal of lightwave technology*, vol. 15, no. 8 pp. 1277–1294, 1997.
- [29] J.E. Sepie, L. Poladian, C. Martijn de Sterke, "Propagation through no uniform grating structures," *Optical Society of America*, vol. 11, no. 4 pp. 1307–1320, 1994.
- [30] D. Marcuse, "Theory of dielectric optical waveguides", New York: Academic, 1991, ch.2.
- [31] H. Kogelnik, "Theory of optical waveguides," in *Guided-Wave Opto-electronics*, T.Tamir, Ed. New York: Springer-Verlag, 1990.
- [32] P.F ernandez, J.C. Aguado, J. Blas, R. Duran, et al, "Optimization of the apodization strength of linearly chirped Bragg gratings for span dispersion compensation," in *Optical and Quantum Electronics*, vol.36, pp. 57-66, 2004.
- [33] K.F. Riley, M.P. Hobson, S.J. Bence, *Mathematical Methods for physics and engineering*, 1st ed., Cambridge University Press, 1998.
- [34] Karin Ennser, Mikhail N. Zervas, and Richard I. Laming, "Optimization of apodized linearly chirped fiber gratings for optical communications," *IEEE Journal of Quantum Electronics*, vol.34, no.5, pp. 770-778, May 1998.

List of Publications

Journal Paper

- [1] **S. S. Azmiri Khan** and M. S. Islam, "Determination of the Best Apodization Function and Grating Length of Linearly Chirped Fiber Bragg Grating for Dispersion Compensation," *Journal of Communication*, June 2012, *in press*.

International Conference Papers

- [1] **S. S. Azmiri Khan** and M. S. Islam, "Chromatic Dispersion Compensation Using Linearly Chirped Apodized Fiber Bragg Grating," *Proc. of the International Conference on Electrical and Computer Engineering (ICECE)*, Dhaka, Bangladesh, pp. 9-12, 20-22 December 2010.
- [2] **S. S. Azmiri Khan** and M. S. Islam, "Dispersion and Dispersion Compensation Using Linearly Chirped Apodized Fiber Bragg Grating," *Proc. of the Conference on Engineering Research, Innovation and Education (CERIE)*, Sylhet, Bangladesh, pp. 899-902, 11-13 January 2011.
- [3] **S. S. Azmiri Khan** and M. S. Islam, "Performance Evaluation of Different Apodization Profiles of Linearly Chirped FBG for Dispersion Compensation," *Proc. of the International Conference on Computer and Information Technology (ICCIT)*, Dhaka, Bangladesh, p. 41, 21-23 December 2011.